International Journal of Coal Science & Technology (2024) 11:39
https://doi.org/10.1007/s40789-024-00680-2

REVIEW

Research advances in enhanced coal seam gas extraction by controllable shock wave fracturing

Chaojun Fan[1] · Hao Sun[1] · Sheng Li[1] · Lei Yang[1] · Bin Xiao[1] · Zhenhua Yang[1] · Mingkun Luo[2,3] · Xiaofeng Jiang[1] · Lijun Zhou[1,2]

Received: 30 December 2023 / Revised: 17 February 2024 / Accepted: 11 March 2024
© The Author(s) 2024

Abstract

With the continuous increase of mining in depth, the gas extraction faces the challenges of low permeability, great ground stress, high temperature and large gas pressure in coal seam. The controllable shock wave (CSW), as a new method for enhancing permeability of coal seam to improve gas extraction, features in the advantages of high efficiency, eco-friendly, and low cost. In order to better utilize the CSW into gas extraction in coal mine, the mechanism and feasibility of CSW enhanced extraction need to be studied. In this paper, the basic principles, the experimental tests, the mathematical models, and the on-site tests of CSW fracturing coal seams are reviewed, thereby its future research directions are provided. Based on the different media between electrodes, the CSW can be divided into three categories: hydraulic effect, wire explosion and excitation of energetic materials by detonating wire. During the process of propagation and attenuation of the high-energy shock wave in coal, the shock wave and bubble pulsation work together to produce an enhanced permeability effect on the coal seam. The stronger the strength of the CSW is, the more cracks created in the coal is, and the greater the length, width and area of the cracks being. The repeated shock on the coal seam is conducive to the formation of complex network fracture system as well as the reduction of coal seam strength, but excessive shock frequency will also damage the coal structure, resulting in the limited effect of the enhanced gas extraction. Under the influence of ground stress, the crack propagation in coal seam will be restrained. The difference of horizontal principal stress has a significant impact on the shape, propagation direction and connectivity of the CSW induced cracks. The permeability enhancement effect of CSW is affected by the breakage degree of coal seam. The shock wave is absorbed by the broken coal, which may hinder the propagation of CSW, resulting in a poor effect of permeability enhancement. When arranging two adjacent boreholes for CSW permeability enhancement test, the spacing of boreholes should not be too close, which may lead to negative pressure mutual pulling in the early stage of drainage. At present, the accurate method for effectively predicting the CSW permeability enhanced range should be further investigated.

Keywords Controllable shock wave · Permeability enhancement · Gas extraction · Basic principle · Experimental test · Mathematical models · On-site test

1 Introduction

With the increase of coal mining in depth, the permeability of coal seam generally decreases, which has a serious impact on the gas extraction efficiency. The effective transformation and permeability enhancement of coal seam is the primary technical problem for ensuring the safety production of coal mine. At present, the main coal permeability enhancement technologies include protective layer mining (Yao et al. 2016), deep hole pre-split blasting (Li et al. 2021), hydraulic fracturing (Chen et al. 2021a; Yang et al. 2023a), and liquid CO_2 fracturing (Fan et al. 2021a). However, these

✉ Chaojun Fan
chaojunfan@139.com

[1] College of Mining, Liaoning Technical University, Fuxin 123000, China

[2] College of Safety Science and Engineering, Liaoning Technical University, Fuxin 123000, China

[3] Energy Business Department, Shanxi Lu'an Chemical Group, Changzhi 046200, China

Published online: 14 May 2024

means have certain limitations. For instance, the construction period of protective layer mining is long limited by the coal seam environment and mining conditions,. Deep hole pre-split blasting demands more boreholes, resulting in the great potential safety hazards in the construction process. Hydraulic fracturing is prone to water plugging and the secondary pollution to coal seams. Liquid CO_2 fracturing, with poor economic benefits, has high requirements for construction technology (Feng et al. 2012; Xiao et al. 2024). The controllable shock wave (CSW), as a newly developed method for enhancing permeability of coal seam in recent ten years, is a pure physical stimulation technology, which does not need to inject other liquids into the reservoir, and is safe and pollution-free. Compared with other coal seam permeability enhancing technologies, the CSW technology is characterized by the following advantages: (1) The CSW fracturing process is simple with reduced engineering cost; (2) It can accurately control the position and intensity of operation; (3) It has multiple and multi-point balanced operation, without damaging the reservoir and avoiding damage to the reservoir; (4) This technology can improve the efficiency and concentration of gas extraction, thereby reducing the emission of gas into the atmosphere during coal seam mining, and preventing air pollution and greenhouse gas effects. But it is still in the experimental stage and has not been widely applied in coal mine field.

Based on the technologies of pulse power and discharge plasma (Qiu et al. 2012), the CSW converts electrical energy into mechanical energy of shock wave. With the repeated operation of pulse power source, the shock wave with controllable amplitude, impulse and action area can be generated in the same location. The discharge process includes two important processes: the phase transition of the spark-over medium and the formation of a plasma channel by spark-over. these processes generate volume expansion and push the water to generate compression waves (Zhang et al. 2019a). After acting on the coal as a cylindrical wave, the shock wave propagates outward through the coal seam (Zhang et al. 2017b). In this process, the strong loading effect of shock wave can transform the fracture structure in coal and improve the permeability of coal seam. The strong elastic wave acting on the coal seam can break the gas occurrence state in the coal seam and promote the desorption of adsorbed gas (Wang et al. 2021). The stronger the strength of the CSW is, the more the number of cracks in the coal is, and the greater the length, width and area of the cracks being (Yan et al. 2016, 2019). After being impacted, the origin of coal crack follows the maximum tensile stress criterion, with mainly tensile damage (Bao et al. 2021), and the damage propagation in coal is related to the impacted times (Zhang et al. 2019a). Under the influence of in-situ stress, the damage of coal mass is restrained, and the form of crack propagation also changes with the strength and direction of in-situ stress (Jia et al. 2022). Gas extraction after the CSW fracturing involves damage-fluid–solid coupling process. The following factors need to be considered: the fracture and pore structure in coal seam (Jigna et al. 2020), the fluid flow in fracture (Lu et al. 2010), the gas diffusion in the coal matrix (Liu et al. 2022), the stress change in reservoir with gas migration (Liu et al. 2020), the influence of damage in coal seam on permeability (Zheng et al. 2017), the impact of water in coal seam on gas migration in cracks (Chen et al. 2021b). When the CSW is applied in the field, based on the degree of coal seam breakage, the parameters of reasonable position (Wang 2020), density (An et al. 2020), strength of CSW impact (Yan et al. 2021) and the spacing of operating boreholes (Su et al. 2021) need to be designed.

With the purpose of better applying the CSW in coal mines, the theoretical analysis, the laboratory experiments and the numerical simulation were conducted, which provide a theoretical basis for enhancing gas extraction in coal seam by CSW fracturing. The theoretical analysis were mainly focused on the generation mechanism of CSW and the enhancing effect of permeability in coals. The impact of discharging and loading parameters on the shock wave generation process was analyzed. The propagation and attenuation law of shock wave in coal seam was studied, the enhancing mechanism of coal seam permeability under the combined action of shock wave and bubble pulsation was analyzed. The development of the CSW fracturing experimental platform provides a technical means for the CSW fracturing samples under the conditions of simulated stress in the laboratory. The influence of impact energy, impact times and in-situ stress on CSW fracturing coal samples can be studied. However, limited by technical conditions and size effect, the laboratory experiment can hardly show the process of the CSW fracturing coal seam. Therefore, the key to studying the CSW fracturing is to use mathematical method to model the governing equations of each physical field in the process and then import them into the numerical simulation. The mainly physical fields include the interactions of damage field, fluid field, solid field coupling with gas–water two-phase. Therefore, the law of gas migration in coal seam after CSW fracturing can be better understood. In this review, it summarizes the research advances on enhanced gas extraction of coal seam by CSW from the perspectives of theoretical analysis, laboratory test, mathematical model and field test, including: (1) The generation mechanism of CSW and the enhancing framework of coal permeability by CSW fracturing; (2) Equipment development and experimental test on coal seam CSW fracturing under different factors; (3) The damage-stress-seepage coupling mathematic model; (4) Technical development of coal permeability enhancement by CSW fracturing, and field tests conducted in China.

2 Research advances in basic principle of coal seam by CSW fracturing

2.1 Generation mechanism of CSW

In the early studies, the CSW was created by the pulse power technology and the electrohydraulic effect, converting the electrical energy stored by the pulse power driving source into mechanical energy of shock wave through high-voltage discharge in water. In order to improve the efficiency of energy conversion, many scholars have conducted systematic researches on the plasma formation process by high-voltage spark-over metal wire (Han et al. 2015; Chao et al. 2014), and developed a CSW technology generated by the electric explosion of metal wires in water (Zhou et al. 2015a, b, c, d). Whether the shock wave is generated by electrohydraulic effect or wire electric explosion, the output energy of the shock wave only comes from the energy stored in the pulse power driving source, which has a limited effect on the coal reservoir, with a small effective operating radius. Based on the electric explosion energy converter, the CSW can excite energetic materials to produce shock waves with higher energy, so that the research and development of electric pulse CSW technology can enter a more practical stage (Liu et al. 2017).

The generation process of shock wave is a complicated physicochemical change process, including the conversion of electrical energy into multiple forms of energy such as mechanical energy, thermal energy and chemical energy, accompanied by some physical phenomena such as phase change, strong light, great sound and large electromagnetic radiation (Sun 2013). The process lasts for a short duration and is highly non-linear, dispersed and unstable (Liu et al. 1999). This paper mainly studies the influence of CSW on the permeability enhancement of coal seam, and merely focuses on the impact mechanical effect of pulse discharge process, without considering the influence caused by electromagnetic and optical radiation effects in the process.

According to different loading media between discharge electrodes, CSW technology can be divided into three types:

(1) Hydro-electric effect: there is only water between discharge electrodes, and the shock wave is generated by high-voltage spark-over of the water, which is referred to as WG in this review. Zhou (2017) analyzed the generation process and mechanism of shock waves in water, and the formation of shock waves by liquid phase transition and plasma channel expansion and compression of water.
(2) Metal wire explosion: a metal wire is loaded between the discharge electrodes to generate shock wave by high-voltage spark-over of the wire, which is referred to as EW in this review. Grinenko et al. (2006) photographed the nanosecond pulse discharge process of metal wire in water at a power of 6GW using shear interferometry, radiometric fluoroscopy and Schlieren photography. The discharge process of metal wire explosion includes two stages: phase transition and spark-over. The former is the process of instantaneous vaporization and volume expansion of metal, and the latter is the process of metal transformation from vapor–liquid mixture to plasma state. In these processes, it will generate volume expansion and push water to generate compression waves, which merge in to form a stronger shock wave in a very short time (Yao et al. 2019).
(3) Excitation of energetic material by wire explosion: a metal bar wrapped with energetic material is added between the discharge clicks, relying on the metal wire explosion and excitation of energetic material to produce shock wave, which is referred to as EMs in this review. For the initiation of energetic materials by wire electric explosion, the electric explosion generally occurs before the chemical reaction, and then the detonation wave sustained by the chemical reaction will enhance the shock wave caused by the phase explosion (Rososhek et al. 2019).

To summarize, under both WG and EW loading conditions, the shock wave is generated by the phase transition of the medium between electrodes caused by high-voltage discharge and the expansion of the plasma discharge channel followed by compression of the water. When the load is EMs, the shock wave generated by the excitation of energetic materials should also be considered. The physical process of shock wave generation under three different media loading conditions is shown in Fig. 1.

Regardless of the media types between the discharge electrodes, the expansion process of plasma channel plays an important role in practical applications. Many scholars have used energy conservation, magnetohydro-dynamics and fluid dynamics to describe the characteristics of discharge channel plasma theoretically, as shown in the Table 1.

Based on the energy balance equation, Li et al. (1994) established the relationship between the discharge power and the rate of internal energy increase in the plasma channel, bubble expansion attack power and radiation power, and calculated the pressure, conductivity, and gap resistance parameters of the plasma channel during the discharge process by means of theoretical derivation, which lays a theoretical foundation for future research. Oreshkin et al. (2007) approximately described the expansion process of plasma channel during metal wire explosion in water by means of the MHD. In the process of generating CSW, when the

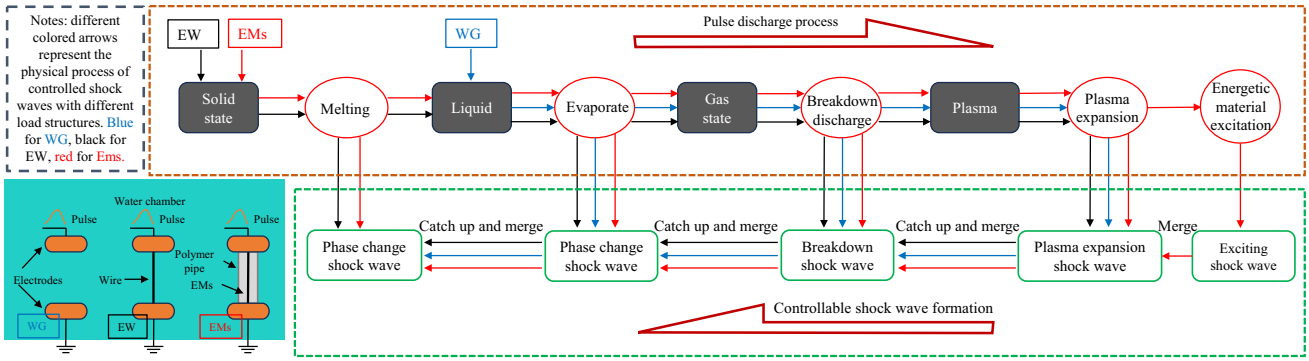

Fig. 1 Physical process of CSW by loading media of WG, EW and EMs

Table 1 Characteristic description equation of typical plasma

Theories	Plasma characterization equations	Variable explanation
Energy conservation (Li et al. 1994)	$E = \frac{1}{\gamma - 1}\frac{\mathrm{d}(PV)}{\mathrm{d}t} + P\frac{\mathrm{d}V}{\mathrm{d}t} + \frac{\mathrm{d}Ra}{\mathrm{d}t}$	where E is electrical power consumed in the discharge channel; γ is the ratio of the specific heat of pressure to the specific heat of volume of gas; P is pressure; V is volume of discharge channel; Ra is the radiant energy; t is time
Magnetohydro-dynamic (MHD) (Oreshkin et al. 2007)	$\frac{\mathrm{d}\rho}{\mathrm{d}t} + \frac{\rho}{r}\frac{\partial(rV)}{\partial r} = 0$ $\rho\frac{\mathrm{d}V}{\mathrm{d}t} = -\frac{\partial p}{\partial r} - j_z B_\varphi$ $\rho\frac{\mathrm{d}\varepsilon}{\mathrm{d}t} = -\frac{p}{r}\frac{\partial(rV)}{\partial r} + \frac{j_z^2}{\sigma} + \frac{1}{r}\frac{\partial}{\partial r}r\left(K\frac{\partial T}{\partial r} - W_\mathrm{R}\right)$ The Maxwell equations, $\frac{1}{c}\frac{\partial B_\varphi}{\partial t} = \frac{\partial E_z}{\partial r}, j_z = \frac{c}{4\pi r}\frac{\partial(rB_\varphi)}{\partial r}, j_z = \sigma E_z$	where d/d$t = \partial/\partial t + v\,\partial/\partial r$ is a substantial derivative, ρ and T are the density and temperature of matter, V is the radial velocity component, p and ε are the pressure and the specific internal energy, W_R is the spectrum-integral radiation flux, c is the velocity of light in vacuum, B_φ is the azimuthal component of the magnetic field strength, E_z is the axial component of the electric field strength, j_z is the axial component of the current density, and K and σ are the thermal and electrical conductivity, respectively
Fluid dynamics (Barbashova et al. 2007)	$\frac{\partial\rho}{\partial t} + v\frac{\partial\rho}{\partial t} + \rho(\nabla\cdot v) = 0$ $\frac{\partial v}{\partial t} + v\frac{\partial v}{\partial r} = -\frac{1}{\rho}\frac{\partial p}{\partial r}$ $\frac{\partial}{\partial t}\left(\rho\left(\varepsilon + \frac{v^2}{2}\right)\right) + \nabla\cdot\left(\rho v\left(\varepsilon + \frac{p}{\rho} + \frac{v^2}{2}\right)\right) = \frac{1}{\rho}\frac{j^2}{\sigma}$	where r is the radial distance; v, ρ and p are the radial velocity of the discharge plasma channel, density, pressure, respectively; σ is plasma conductivity; j is discharge channel current density; ε is plasma energy

discharge plasma channel is formed with an approximately shape of axisymmetric cylinder, which is the most widely used equation for describing plasma characteristic at present. But, its calculation process is cumbersome and inconvenient to use. Barbashova et al. (2007) studied the hydrodynamic process of pulsed discharge in water by means of numerical calculation. When the power supply of pulse discharge is fixed, a higher expansion velocity, channel pressure and specific momentum can be obtained by selecting the parameters of the oscillating discharge mode. According to the experimental results of Sasaki (Sasaki et al. 2006), the radial distribution of plasma channel parameters formed during the electric explosion of metal wires in water is relatively uniform. Based on this discovery, Chao et al. (2014) simplified the hydrodynamic equation and established a simple 0-dimensional numerical model of plasma characteristics in water. The initial state of the plasma channel is estimated by the combination of the ideal gas equation of state, the Tucker resistivity-specific action equation and Sariksov 0-D thermodynamical equation.

The above is the theoretical study about the expansion process of plasma channel to form CSW under high-voltage spark-over, in which the shock wave is generated by expansion and compression of water in plasma channel. In the experiment, the empirical formulas of shock wave pressure was obtained through the monitoring of shock wave pressure and velocity in the process of shock wave propagation. The influence of spark-over voltage and propagation distance, as well as the wire parameters and energetic materials, on the induced CSW was revealed.

By studying the relationship between discharge energy parameters and shock wave pressure and velocity in the

process of pulse discharge, Zingerman (1956) proposed a formula for calculating the peak pressure of shock wave.

$$P_{\mathrm{M}} = \beta\sqrt{\frac{\rho_0 W}{\tau T}} \tag{1}$$

where P_{M} is the maximum wave front pressure of pulse discharge shock wave; β is the dimensionless complex integral function; ρ_0 is the density of water; W is the total pulse energy per unit length of the discharge channel; T is the duration of pulse discharge energy; τ is the wave front time. It can be seen that the peak pressure of shock wave generated by pulse discharge in water is directly proportional to the density of water and the electrode discharge energy, and is inversely proportional to pulse duration and wave front time.

Lu et al. (2002) used a high-speed camera and pressure sensor to monitor the pressure characteristics of shock wave during pulse discharge in water. The peak pressure of shock wave is obviously dependent on the discharge voltage and electrode gap. When the electrode gap is small, the discharge voltage has slight effect on the peak pressure, while when the gap is large, the increase of discharge voltage will significantly increase the peak pressure of the pulse discharge shock wave.

Shock waves with peak pressures can be obtained in the central explosion area, and this pressure can be attenuated to several megapascals at distances of tens of centimeters from the explosion center (Maurel et al. 2010; Zhou et al. 2016; Grinenko et al. 2005). Based on the fluid dynamics theory, Sultanov and Oleinikov (1976) qualitatively calculated the relationship between the shock wave pressure amplitude and the distance. Touya (2006) measured the peak pressure of the generated shock wave, and the experimental device is shown in Fig. 2. The Fig. 3 shows the relationship between the discharge voltage and the peak pressure of the shock wave measured by the experiment, and the empirical expression of the peak pressure of the shock wave and the spark-over energy of the high-voltage pulse can be summarized:

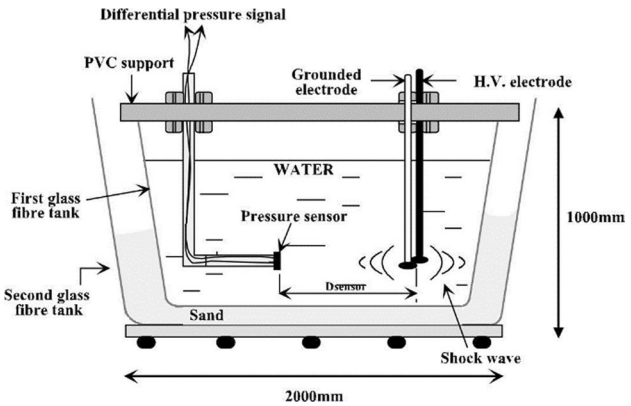

Fig. 2 Schematic diagram of Touya's experiment device for high pulsed discharge in the water. (Touya et al. 2006)

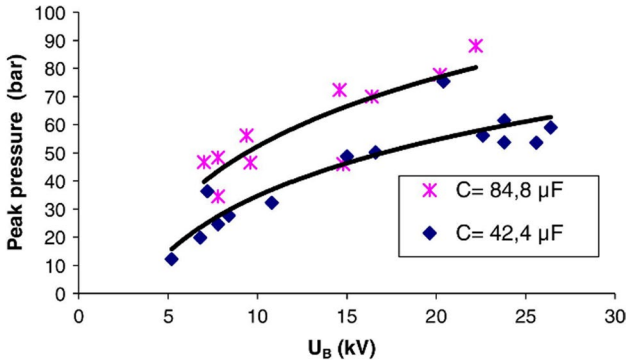

Fig. 3 Relationship between peak pressure of shock wave and spark-over voltage. (Touya et al. 2006)

$$P_{\mathrm{m}} = hE_{\mathrm{B}}^{\alpha} \tag{2}$$

where E_{B} is the energy at the time of spark-over; P_{m} is the peak pressure of shock wave; h and α are the attenuation coefficients of shock wave propagation; h is the inverse proportional function of the propagation distance; α is related to the electrode type and spark-over voltage. The relationship among spark-over energy E_{B}, spark-over voltage U_{B} and energy storage capacitance C can be expressed as:

$$E_{\mathrm{B}} = \frac{1}{2}CU_{\mathrm{B}}^2 \tag{3}$$

Increasing the stored energy can improve the shock wave intensity, and under the same stored energy, the shock wave intensity can be improved by changing the energy conversion rate between the metal wire parameters in the water. It is found that the phase transition process of the metal wire contributes significantly to the shock wave, and the size and material of the metal wire have a significant impact on the intensity of the shock wave.

Tucker et al. (1961, 1975) studied the relationship between the specific action and resistivity of more than 20 kinds of commonly used metals by experiments, calculating the energy required for the melting and vaporization of these commonly used metals in the explosion process by using the collected data, and gave the calculation model of the electrical explosion energy of metal wires.

Although there is no obvious difference in the phase evolution of different metal wires in the process of metal wire explosion, the intensity of shock wave is significantly different due to the different channel expansion trajectories (Han et al. 2018). Wires made of low melting point metals can usually produce strong shock waves, among which Cu and Al can produce the strongest shock waves. The high melting point wire has a large amount of energy for gasification, leading to a weak shock wave energy. The metal with more active chemical properties reacts with water in the process

of electric explosion, which formed strong light radiation, resulting in low efficiency of the shock wave energy conversion. The wire size will affect the wire gasification. Hao (2019) found that with the increase of wire diameter, the injection rate of energy decreases, but the energy injected into the wire increases. The wire material will also have an important impact on the wire explosion process, finding that the energy utilization rate of copper wire is higher than that of aluminum wire. Shi et al. (2021a) carried out electrical explosion experiments of copper wire in water to study the influence of wire size on the propagation process of shock wave. The change of the diameter and length of the metal wire will significantly affect the discharge mode in the process of electric explosion. The shock wave produced by the long metal wire has a small near-field peak value, a small attenuation index, and a slow attenuation during the propagation process, but with a large far-field peak value. The researches have shown that in order to achieve the strongest shock wave under the same discharge energy storage conditions, it is necessary to increase the length and diameter of the metal wire as much as possible to improve the quality under the premise of ensuring the complete gasification of the metal wire (Grinenko et al. 2006). However, with a too large metal wire size, the diameter is prone to be uneven. When the metal wire with uneven thickness explodes, the part with smaller diameter of the metal wire will form a plasma sheath, so that the part with larger diameter will no longer have electrical explosion, which inhibits the growth of shock wave energy (Hollandsworth et al. 1998). It can be concluded that under the same discharge energy storage conditions, there is a problem about wire size parameter matching in wire electrical explosion.

There have been widely used about the wire electric explosion, such as initiating explosive and ignition precursors (Li et al. 2007; Jin 2014), which has also been used to improve the conversion efficiency of the shock wave energy and solve the problem of low shock wave energy under the action of the other two loads in the technology of CSW fracturing coal seam. As for the energetic materials with low energy release rate, the shock wave generated by excitation has a long catch-up process. When the size of energetic load is small, the shock wave generated by energetic materials and the shock wave generated by electric explosion of metal wire can hardly combined in time. Generally, the two separate shock waves with insufficient intensity can be observed (Han et al. 2015).

At present, there are mainly two types of energetic materials used for the coal seam by CSW fracturing: (1) One is the energetic material, which is a mixture of nitromethane, aluminum powder, and copper oxide powder, and is driven by tungsten wire electric explosion. It is also found that when 2.8 g of this energetic material is added, the amplitude and energy of the shock wave in the underwater wire electric explosion increase by 1.7 and 7.9 times respectively (Shi et al. 2021b). (2) The other is the aqueous suspension prepared from nanoscale aluminum powder, which is easier to be obtained compared with other general energetic materials (Rososhek et al. 2019). Krasik et al. (2012) used the electric explosion to cause rapid phase transition of metal wires and then to form a dense plasma with a high temperature up to several electron volts to detonate aluminum powder suspension, this method allows aluminum micro-particle combustion in the estimated range of 32%–79% efficiency.

The ratio of shock wave mechanical energy and the stored electrical energy is the energy conversion efficiency. In order to obtain three different types of energy conversion efficiency generated by shock wave, there are a lot of studies done by the predecessors. Cook et al. (1997) studied the dynamic characteristics of bubbles during pulse discharge in water, the migration of energy flow and mass flow during bubble growth and the bubble impact process, and qualitatively analyzed the acoustic efficiency by shock wave conversion. VanDevender (1978) uses the Martin's semi empirical formula to describe the dissipation relationship between discharge current and discharge energy. The energy conversion efficiency of pulse discharge in water is 5%–11%. Grinenko et al. (2006) analyzed the wire explosion process in combination with the principles of optical images and fluid dynamics, and estimated that the conversion efficiency from electrical energy to shock wave mechanical energy during pulse discharge of wire in water is about 15%–24%. The above research is only for the shock wave energy conversion of WG and EW under specific conditions, and cannot represent all cases. The energy conversion under the three load conditions needs further study.

2.2 Mechanism of coal permeability enhancement by shock wave fracturing

The fracturing process of coal mass by CSW in water is similar to that caused by explosive explosion in water, because the rapid expansion of plasma channel in the process of CSW discharge is equivalent to an explosion source (Xun et al. 2010). The explosion of explosive will generate high-temperature and high-pressure explosive gas. In the generation of CSW, the release of energy will instantly vaporize and ionize water, resulting in bubble pulsation (Yan et al. 2014; Hu et al. 2021). The intensity of bubble pulsation is similar to that of high-temperature and high-pressure explosive gas produced by explosives (Gao et al. 2003; Li et al. 2019b). It is helpful to understand the principle of CSW fracturing of coal mass by reference to the relevant research theories of rock blasting.

During the implement of CSW fracturing in the boreholes of coal seam, the shock wave acts on the coal as a cylindrical

wave and propagates outwards through the coal seam. When the shock wave propagates in the coal seam, it works on the reservoir and destroys the coal structure, as consuming energy and decaying. As shown in Fig. 4, the evolution law of shock wave attenuates from shock wave to stress wave and then to elastic wave when it propagates in coal seam. Therefore, with different distance from the borehole, the mode of action of shock waves on coal seams, as well as the effect of enhancing permeability correspondingly varies.

In the area around the borehole, the intensity of shock wave is the largest. When its amplitude exceeds the tensile strength of the coal seam, it can directly fracture the coal seam. The fracturing degree of coal mass is related to the amplitude and impulse of shock wave. When the amplitude and impulse of the shock wave are strong enough, it will squeeze the surrounding coal seam to form a cavity and form a high-density shell at the outer edge of the cavity. When the amplitude and impulse of the shock wave decrease, the coal seam forms a broken zone, which can cause collapse of borehole wall, as is called the near zone of electric pulse action. In this area, it is necessary to control the amplitude and action area of the shock wave. On the premise of protecting the structure of the coal seam and drill hole, it is ensured the formation of a crack grid around the borehole to connect the borehole with more coal seams. After part of the coal seam fractured by shock wave, its strength attenuates into a compressive stress wave, whose amplitude is lower than the compressive strength of the coal seam, but still higher than the tensile and shear strength of the coal seam. At this stage, the area where the shock wave reaches may cause the coal seam to form shear and tear cracks in many directions, which is called the middle area of electric pulse action. The shock wave continues to propagate in the coal seam and further attenuates into an elastic wave, whose amplitude is lower than the tensile and shear strength of the coal seam. The elastic wave generates shear force at different interfaces, which can dredge the pulverized coal attached to the surface of the seepage channel of the coal reservoir, called the far area of electric pulse action. Under the strong disturbance of high-intensity elastic wave, the mining coal seam can improve the capillary force and the adsorption retention effect of the even electric layer, reduce the surface tension, improve the seepage capacity of the reservoir, and promote the desorption of adsorbed gas (Wang et al. 2021). The desorption effect of high-strength acoustic wave on reservoir demonstration has been proved by many studies. According to the study of high-strength acoustic wave acting on reservoir rocks (Vahitov et al. 1993), the effective action threshold is 1 kW/m^2. After studying the influence of elastic wave on coal seam permeability and gas adsorption performance (Jiang et al. 2008; Li 2010), it put forward that after loading elastic wave on the coal seam, the desorption law remains unchanged with the increase of the desorption amount.

The bubble pulsation, which produced with the shock wave, propagates more slowly than the shock wave (Oshita et al. 2013). The quasi-static stress field generated by the bubble pulsation acts on the coal mass together with the stress wave (Li 2022). The bubble pulsation will wedge into the existing cracks, whose powerful expansion effect will also push the water in the borehole into the existing cracks at the same time, forming a water wedge effect, which will further expand the cracks. In the corner zone of electric pulse, the force effect of stress wave and water wedge is greater than the dynamic tensile strength. When the comprehensive stress effect of electric pulse wave is equal to the dynamic tensile strength, the crack in coal stops expanding. In this process, the radial stress wave pressure causes the radial expansion cracks in coal mass. The elastic potential energy accumulated in the coal mass acts on the coal mass in the form of unloading wave, resulting in circumferential cracks in the coal. The gas in the original cracks will also act on the existing cracks under the disturbance of electric pulse wave, forcing the fracture further extend and develop. Such circumferential cracks, radial cracks and some irregular cracks make the coal mass form a complex crack network. When the intensity of shock wave decays to zero, the primary action of the CSW ends. By referring to the blasting mechanism of coal, the mechanism and process of coal mass

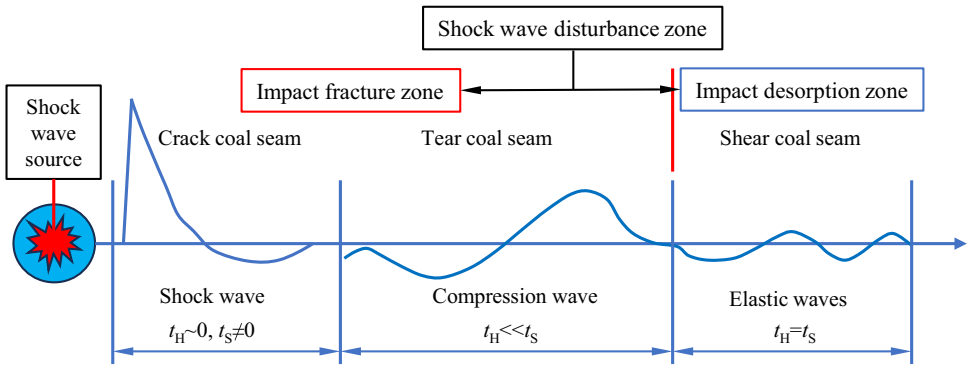

Fig. 4 Schematic diagram of shock wave attenuation law (Zhang et al. 2017c)

t_H-Medium state change time; t_S- time of the state of the medium returns to static

fracturing by high-voltage electric pulse wave are shown in Fig. 5.

The following fracture shock is the repetition of a high-voltage electrical pulse. Under the action of alternating load, even if the stress is lower than the yield strength, the coal will fracture after several cycles. The coal seam is a continuous medium material on the macro level, and produces a large number of bedding, joints and fissures on the micro level. When multiple shock waves act on coal seam, each action is a fatigue process for the next action. The repeated electric pulse will cause fatigue damage to coal mass, further increasing the impact cracking effect of high-voltage electric pulse on coal mass, which expands the complex fracture network of coal mass.

3 Research advances in experiments of coal seam CSW fracturing

3.1 Experimental device

The experiments in laboratories play a crucial role in studying the mechanism of coal seam CSW fracturing, which can effectively reflect the effect of CSW on coal seam, and provide guidance for field tests. At present, the key components of experimental equipment for CSW in laboratories have been studied and developed, mainly including high-voltage pulse power supply, electric spark switch and transmission cable. For the generation devices of CSW, Kovalchuk et al. (2010, 2013) developed two portable high-voltage pulse generators with high output power and operability. Peng (2016) designed a three-electrode gas switch, which optimized the working mode of the spark switch and effectively extended the service life of electrode. In terms of the data monitoring for CSW, Ji et al. (2012) developed high-voltage pulse transmission cables. Chen et al. (2013) developed a high-voltage pulse testing system based on the optical fiber transmission, which optimized the anti-interference ability of the testing system and ensured the non-distortion of long-distance transmission. All of the above researches provide the technical support for the development of experimental platforms in laboratory.

There are many scholars developing a pulse discharge fracturing experimental platform and having achieved some advances. The experimental device developed by Li's team is mainly composed of four parts: water pipe, CBM well casing, electric pulse generator and shock wave pressure sensor, as shown in Fig. 6. The electric pulse generator is composed of the power control cabinet, the high-voltage residual power supply (transformer), the energy storage capacitor, the energy controller and the energy converter. The discharge voltage of the experimental device is 18–20 kV, with the current of 20–30kA. The shock wave pressure sensor, which can measure the maximum pressure of 69 MPa, is produced by the PCB Corporation of the United States (Li 2015). However, this device mainly studies the impact effect of

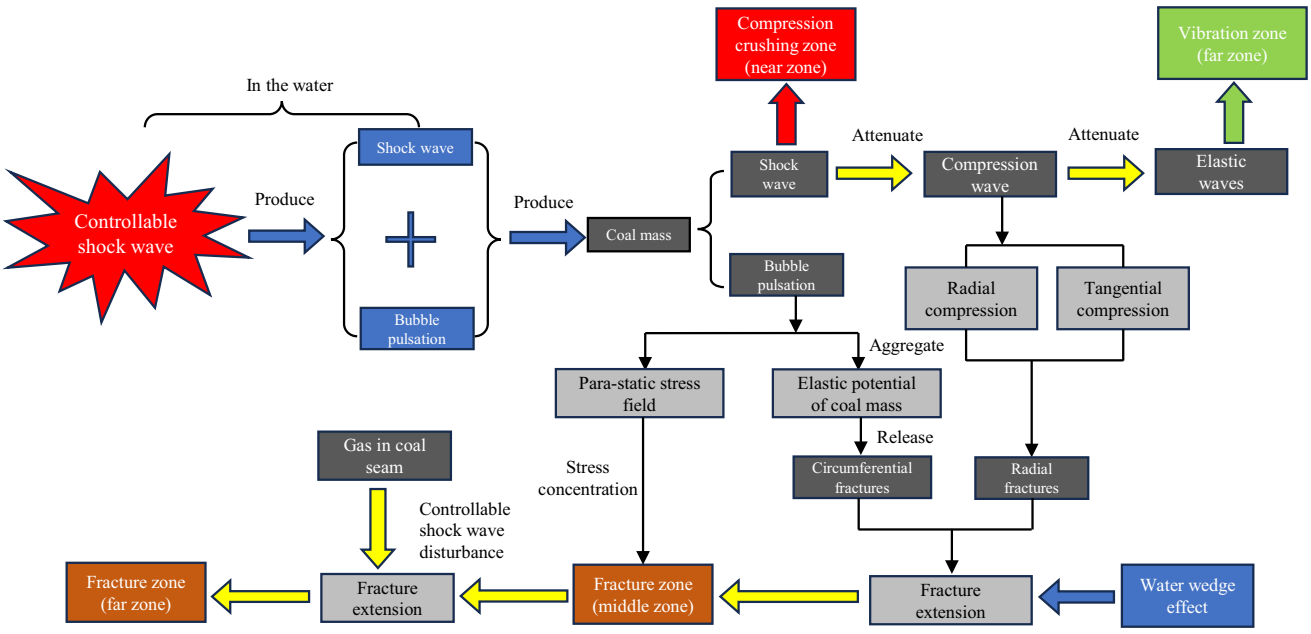

Fig. 5 Mechanism and process of coal mass fracture caused by CSW (Li 2022)

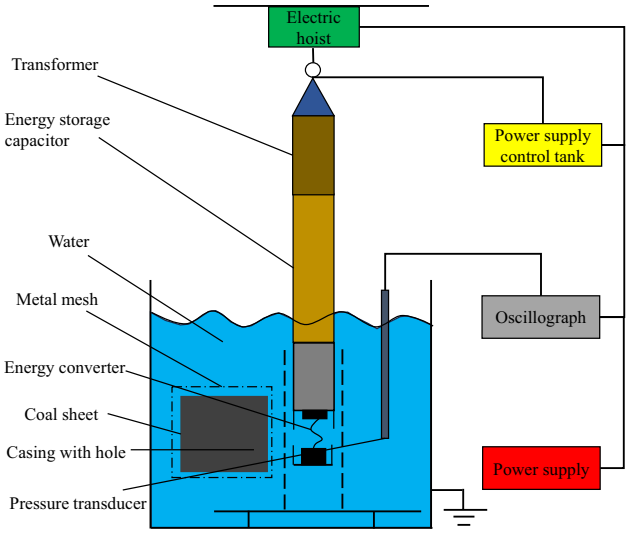

Fig. 6 Experiment platform of electrical pulse stress wave to crack coal samples (Li 2015)

shock wave on coal. As for the pulse discharge experiment conducted on coal in an open environment, it can hardly simulate the fracturing of coal caused by CSW in drilling well (Zhou et al. 2015c; Li et al. 2015).

The experimental platform of the pulse discharge fracturing is based on the interior experimental equipment (Zhou et al. 2015c; Liu et al. 2017) designed for the CSW generator used in field operations, as shown in Fig. 7. This experimental equipment is mainly composed of the control system, the pulse capacitor, the switch, the cable and the shock wave generator, whose working principle is to charge the pulse capacitor through the control system. When the energy storage of capacitor reaches the set value, it will output the trigger signal to drive the gas switch to turn on, release the energy stored in the pulse capacitor through the cable in a very short time, and generate a strong current of 20–100 kA flowing through the loading media to drive the load electrically explosive, and produce strong shock wave to crack the sample (Yang et al. 2020). The experimental device simulates the operation mode of downhole drilling by injecting water on the coal samples, and then inserts the discharge electrode in the borehole to conduct pulse discharge fracturing (Fu et al. 2016; Zhou et al. 2014; Lu 2015).

However, the above two experimental methods basically don't meet with the condition of simulating the confining pressure and loading hydrostatic pressure around the drilling hole. Therefore, in order to improve the experimental conditions, the experimental specimens are pressurized to simulate different stress environments. As shown in Fig. 8a, the Institute of Electrical Industry of the Chinese Academy of Sciences adopted the pulse discharge fracturing experiment of the specimen in the pressure kettle to apply the stress to the coal rock specimen, so as to better simulate the underground engineering implementation conditions of the borehole. Researchers in France have developed a set of experimental device for pulse discharge fracturing and permeability enhancement, in which the principle stress is applied to the top hydraulic cylinder and confining pressure is loaded with lateral constraints (Li 2011; Chen et al. 2012), as shown in Fig. 8b. These two devices can achieve that the test specimen is still in the pseudo-triaxial stress state under the same confining pressure state, and the case of independent hydrostatic pressure applied in the drilling hole is not considered (Sun et al. 2015).

In order to better simulate the in-situ stress and hydrostatic pressure of coal and rock mass in strata, Bian (2018) developed a pulse discharge test-bed composed of the high-voltage pulse discharge system, the hydrostatic loading system and the true triaxial confining pressure loading system. The high-voltage

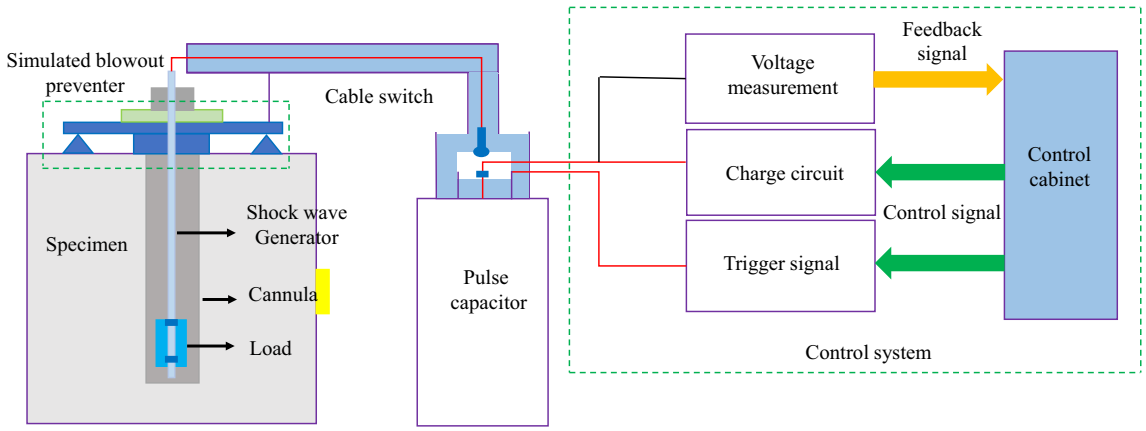

Fig. 7 Experiment platform of electrical pulse stress wave to crack coal samples. (Zhou et al. 2015c)

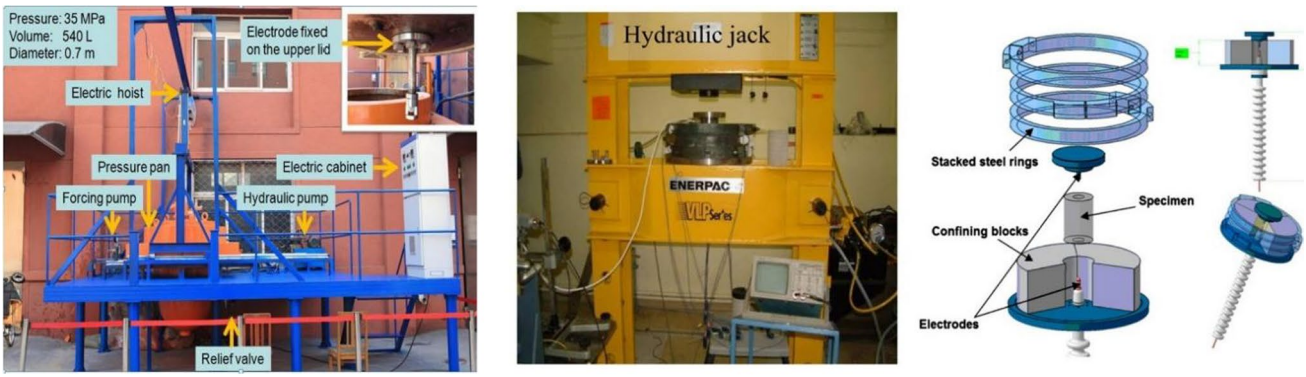

(a) Institute of Electrical Engineering, Chinese Academy of Sciences

(b) University of Pau, France

Fig. 8 Overall view of the test set-up (Li 2011; Chen et al. 2012)

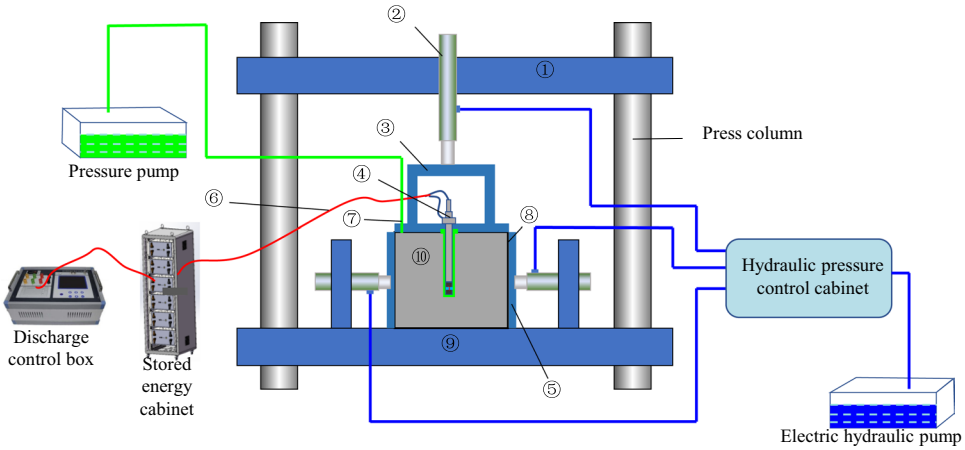

Fig. 9 Working principle of the high-voltage pulsed discharge fracturing test (Bian 2018)

pulse discharge system, as shown in the Fig. 9, is responsible for converting the stored electrical energy into shock wave mechanical energy through the discharge electrode and applying it to the pre-cracked coal and rock samples. The hydrostatic loading system is responsible for providing initial hydrostatic pressure for the specimen drilling. The loading system can apply true triaxial confining pressure to the specimen through hydraulic cylinder, electric hydraulic pump, hydraulic pipeline and other components to simulate the in-situ stress of coal mass in the stratum.

To sum up, the experimental equipment for CSW fracturing has been continuously improved from the aspect of geological environment simulation, which can not only more effectively simulate the real environment of CSW discharge in underground boreholes, but also provide experimental technical support for the study of the CSW effect on coal fracturing under different factors. The experimental set-ups were summarized in Table 2.

3.2 Experiments on coal fracturing by shock wave under different influencing factors

The laboratory experiment is an effective means to study coal fracturing by the high-voltage electric pulse. In experiments, permeability, number of cracks and porosity are usually used as the criteria for determining the effectiveness of fracturing. The measured parameters and calculation methods in these experiments are shown in Table 3. At present, the scanning electron microscopy (SEM) and the mercury intrusion porosimetry (MIP) have been used to analyze the pore structure of coal samples before and after the actions of CSW. The experiments show that the accumulated pores in the coal samples after being treated increase significantly. After being treated, it promotes the expansion and penetration of micro and macro pores and fractures in coal, which improves the permeability of the coal seam and verifies the effectiveness of the CSW on the coal fracturing (Li et al. 2022a; Yan et al. 2019). Chen et al. (2012) conducted an

Table 2 Experiment platform of electrical pulse stress wave for fracturing coal samples

Conducted by	Size of coal sample	Features and advantages	Disadvantages
Li (2015)	Cube with 20 cm × 20 cm × 20 cm	Coal samples placed in water in an open environment	Shockwave energy acts less on the sample and consumes more impact times
Zhou et al. (2015c)	Cylinder with diameter of 1 m and height of 1 m	Sample size is large, and the discharge shock energy is high, which can simulate the CSW fracturing	Generally applicable to concrete specimens, the sample size is not suitable for conducting experiments with coal
Scholar from France (Li 2011; Chen et al. 2012)	Hollow cylinder with inner diameter of 5 cm, external diameter of 12.5 cm and height of 18 cm	Center hole of the sample is subjected to shock, and radial and axial pressure are applied to the sample, which can simulate stress environments of different burial depths	Static water pressure inside the hole cannot be controlled
Bian (2018)	Cube with 30 cm × 30 cm × 30 cm	Apply triaxial stress to the specimen to simulate a true triaxial stress environment and control the initial hydrostatic pressure inside the discharge borehole	Due to the small size of the sample, extremely high requirements are placed on the discharge electrode and experimental setup

Table 3 The measured parameters and calculation methods in these experiments

Parameter	Calculation method
Permeability	Gas injection seepage experiment
Number of cracks	CT scanning and grayscale recognition
Porosity	Scanning electron microscopy (SEM) and Mercury intrusion porosimetry (MIP)

experiment of pulse discharge in water in a rectangular tank, and the experimental device is shown in Fig. 8b. The maximum discharge voltage is 40 kV, the capacitor capacitance is adjustable in the range of 5.3–84.8 μF, and the discharge spacing is 10 mm. The internal cracks and permeability of cylindrical concrete samples before and after discharge were observed and compared, the result is shown in Fig. 10, and it was found that the increase of peak pressure of shock wave and the increase of shock frequency were conducive to the increase of permeability of concrete samples.

However, due to the limitations of the experimental means, the size of coal samples and the simulation conditions of in-situ stress, it can only conduct experimental research on small-size coal sample by CSW with low energy, which can qualitatively study the fracturing effect of CSW in coal, so as to deduce the fracturing effect in field test and design a reasonable construction scheme. In this review, it will summarize the laboratory experiments about CSW from three aspects: the energy of CSW, the shock times and the in-situ stress conditions.

3.2.1 The energy of CSW

The resulting crack pattern and distribution vary with intensity of shock wave, as the shock wave attenuates in the process of propagation in coal mass. When the intensity of shock wave is smaller than the tensile and shear strength of the coal seam, the crack may not occur in the coal seam. When the shock wave intensity is larger than the tensile strength, the cracks are mainly caused by tensile pattern. When the shock wave intensity is greater than the compressive strength of the coal seam, there will be obvious crushing zone around the borehole in coal seam caused by compressive pattern. The larger the shock wave intensity is, the farther the propagation distance is, and the larger the distribution range and number of cracks around the coal seam borehole are.

When the intensity of shock wave exceeds the threshold value, the damage occurs in the coal seam as well as the permeability of the coal sample increases (Chen et al. 2012). The intensity of CSW is determined by the mechanical energy released by high-voltage discharge. With the increase of shock wave energy, the number of cracks, as

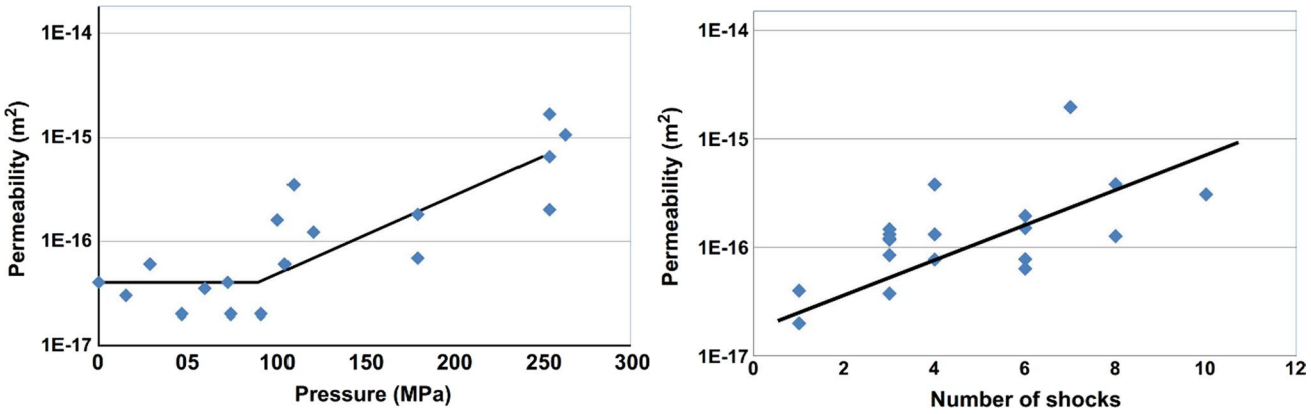

Fig. 10 The relationship between the permeability of concrete specimens and the shock wave's peak pressure and impact times (Chen et al. 2012)

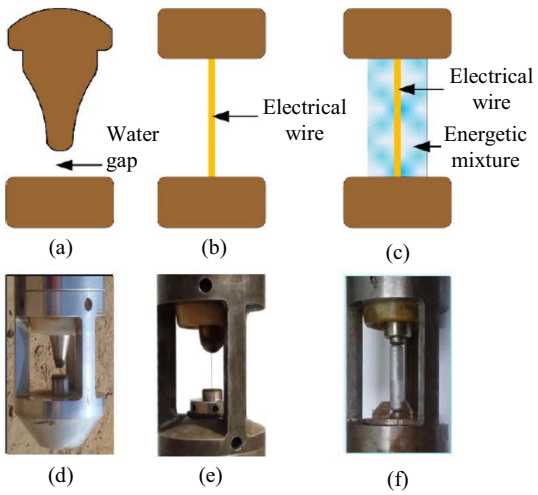

Fig. 11 Structures of three loads: **a** WG load **b** EW load and **c** EMs load: **d** hardware of **a**; **e** Hardware of **b**; **f** Hardware of **c** (Zhou et al. 2015c)

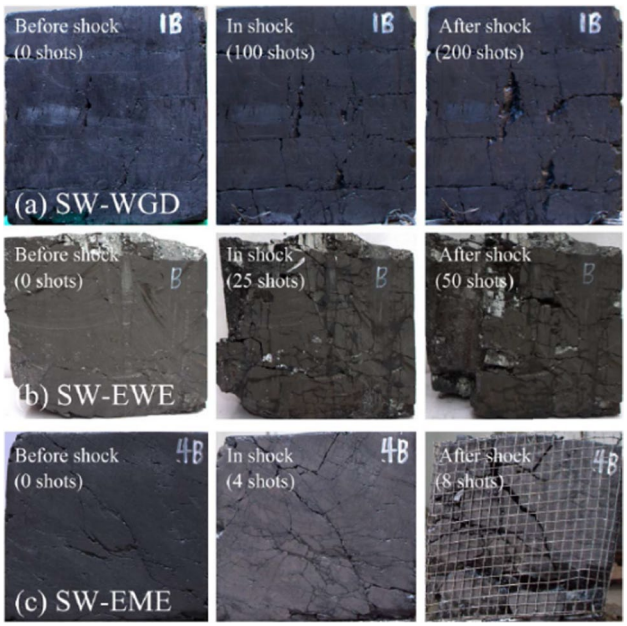

Fig. 12 Fracturing photos of WG discharge (WGD), EW explosion (EWE), and EMs explosion (EME) (Zhou et al. 2015c)

well as the length, width, and area of cracks in the coal increases accordingly (Yan et al. 2018, 2016). Zhang et al. (2023a, b) took the large coal sample of Bailongshan Coal Mine in Yunnan Province as an example to conduct the experiment about the energy optimization by shock wave. Compared with the sample shocked by metal wire and energetic material under the same energy storage condition, the pressure peak and pulse width of the shock wave generated by energetic material were significantly greater than that of metal wire's, with stronger energy and better impact effect. It requires less impact times to achieve the same shocking effect, which is more suitable for shock wave operation in underground coal mine under the actual situation. Zhou et al. (2015c) conducted a comparative experiment on coal crushing with the three load forms of CSW. In Fig. 11 and Fig. 12, it presents the fracturing effects of the three load forms based on pulse discharge. The loading mode of energetic materials excited by metal wire explosion can not only convert the high-voltage electrical energy into the mechanical energy, but also stimulate the chemical energy of energetic materials. Therefore, the shock wave excited by EMs loading has stronger energy, with higher degree of coal fragmentation and less impact times.

3.2.2 Impact times

A large number of experiments have proved that the damage propagation of coal is related to the impact times of CSW (Zhang et al. 2019a). Yang et al. (2020) and Li et al. (2022b) applied the CSW fracturing to the casing perforation

of the cement rock sample, and explored the influence of the impact times of CSW on the fracture morphology and mechanical parameters of the sample. With the increase of impact times, the main crack of the sample becomes wider and longer, and a large number of irregular secondary cracks are generated around it, forming a complex network fracture system. With the increase of impact times, the internal damage of the sample continues to accumulate as well as the mechanical properties of the rock weaken gradually. Zhao (2022) analyzed the crack development law of coal samples with different scales by shock wave. The variation characteristics of permeability of coal samples before and after impact load were studied, and the quantitative relationship between impact times and permeability was established. In the range of shock wave impact, the damage of coal and the crushing of mechanic was obviously observed. The permeability of coal is enhanced after impacted by shock wave. Chen et al. (2012) simulated the influence of dynamic load impact on damage and permeability of mortar and rock sample under different buried depths through laboratory tests of static load system, observing that the accumulation of damage is proportional to the impact times. Zhou et al. (2015d) carried out the pulse load test and the micro scanning observation for metabituminous coal samples, analyzing the main causes affecting the initiation and propagation of micro cracks in coal reservoirs in Ordos region. It was found that when pulse load was applied repeatedly, the frequency of electric pulse discharges was positively proportional to the linear density of micro-cracks. There is an optimal range about the influence of CSW energy on fracturing effect. Overloading will damage the coal reservoir structure, resulting that the crushed pulverized coal increases the wave impedance and the attenuation during shock wave propagation, limiting the expansion of fracturing radius (Qin et al. 2021).

3.2.3 In-situ stress conditions

The effect of underground stress on CSW fracturing coal seam is similar to that of deep coal and rock blasting. As for the effect of in-situ stress on blasting impact, Kutter and Fairhurst (1971) found that the radial cracks generated by blasting would preferentially expand along the direction of the maximum principal stress. Mu (2012), Mu and Pan (2013) believed that the in-situ stress can inhibit the expansion of explosive fractures. Chen et al. (2009) put forward that the in-situ stress was the main reason for the reduction of the proportional radius of the explosive fracture zone, and the lateral pressure coefficient dominated the distribution of the explosive fracture along the circumference of the hole wall, which was consistent with the result obtained by Tao et al. (2020) through numerical simulation. Yang and Ding (2018), and Yang et al. (2019) conducted the dynamic caustics experiment under static loading, and found that, the propagation direction of the explosive crack was mainly controlled by the direction of the prefabricated crack in the initial stage, and the crack gradually deflected towards the loading direction under the influence of static stress in the later stage. In addition, with the gradual increase of in-situ stress, the destruction characteristics of surrounding rock under explosion load will also change (Lu et al. 2012). Zhang (2017a) found that radial crack propagation was suppressed by confining pressure, which reduces the range of fracturing. However, when the confining pressure increased to a certain extent, it promoted the reflection tensile fracture of the specimen. Xiao et al. (2019) believed that the in-situ stress promoted the accumulation of elastic strain energy in the surrounding rock. Under the action of explosion load, the elastic zone of the surrounding rock evolves into a damage and destruction zone, which expanded the range of rock fracturing.

Bian (2018) designed the crack propagation experiment of impact cracking cement under different stress conditions of three axes, and the experimental results are shown in the Fig. 13. Where σ_1 represents the axial stress, σ_2 represents the stress in the SN direction, and σ_3 represents the force in the EW direction. The effect of ground stress on the cracking effect is obtained by comparing the test results. With the increase of in-situ stress, there are critical values for crack radius and degree of fracture. The difference in horizontal principal stress has a significant influence on the shape, propagation direction, and connectivity of CSW induced cracks (Qin et al. 2021).

4 Research advances in modeling of enhanced gas extraction by CSW fracturing

4.1 Damage model

The principle of CSW fracturing is similar to that of traditional explosive blasting, both of which use the shock wave generated by the conversion of energy to destroy the surrounding rock mass. The high-voltage discharge produces a strong wave in a very short time to blast the rock, and the shock wave propagates in the coal and rock. The undisturbed coal and rock mass contains tiny cracks, holes and other original damage. When the loading stress on coal and rock exceeds their yield limit, the original damage in coal and rock mass will further expand and extend until it penetrates the whole coal and rock mass. In this process, new cracks will be continuously generated, which plays an important role in promoting the whole damage of rock mass. Dougill et al. (1976) initially proposed the application of damage mechanics in the study of rock material mechanics as the research basis for the damage mechanism and basic theory of rock mass under different circumstances. Scholars

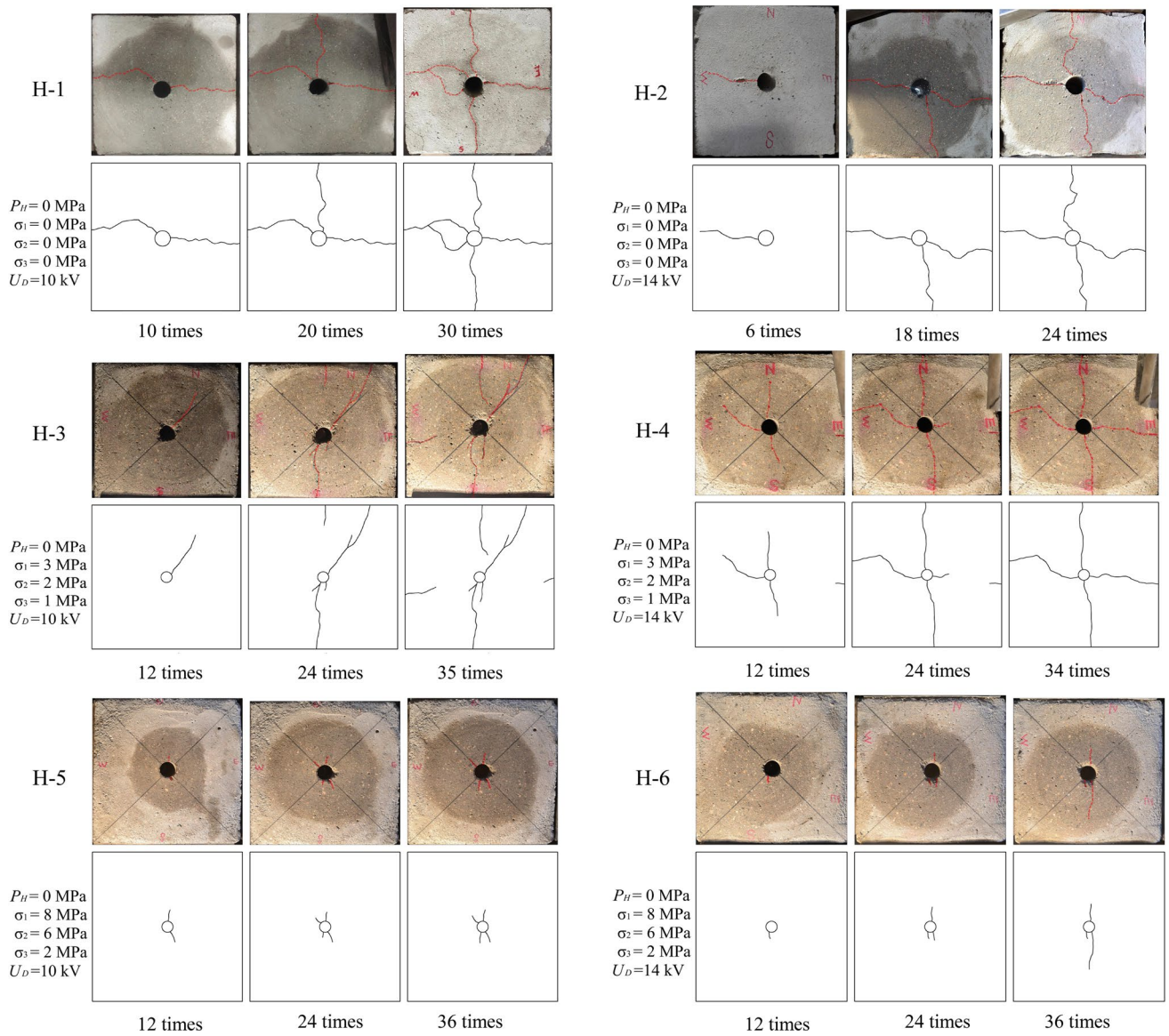

Fig. 13 The cracks' propagation of pulsed discharge fracturing under different in-situ stress (Bian 2018)

proposed the damage models under different conditions. By analyzing the damage process from the perspective of damage mechanics, it can be quantitatively evaluated about the damage changes of rock mass at macro and micro levels through numerical values, such as the macro and micro damage variables, so as to intuitively and vividly characterize the damage process of coal and rock mass under shocks.

The representative damage models include the G-K damage model and the TCK damage model:

4.1.1 G-K damage model

Grady and Kipp (1980) hypothesized that there are a large number of primary cracks with random distribution of length and spatial in the rock mass, most of which follow the two-parameter Weibull distribution. The damage coefficient is introduced to demonstrate the average fragment size of the rock which is damaged during the crushing process, so as to predict the approximate size of the damaged rock. When the rock is subjected to the external loads, the crack activation number inside the rock follows the two-parameter distribution of the volume tensile strain:

$$n(\varepsilon) = k\varepsilon^m \tag{4}$$

where, ε is the volume strain; k and m are the coefficients of the medium.

From Eq. (4), it is deduced that the activation rate of crack is:

$$N = km\varepsilon^{m-1}\varepsilon_x\left(1 - D_x\right) \tag{5}$$

where, D_x is the reduction coefficient of rock strength caused by fracturing; ε_x is the strain rate.

The expression of damage in the rock is:

$$D = \frac{4}{3}\pi C_8^3 km \int_0^t \varepsilon^{m-1}\varepsilon_x\left(1 - D_x\right)(t-\tau)^2 \mathrm{d}\tau \tag{6}$$

where, t is the time when the rock is subjected to stress; τ is the response time. Then, the total damage area and the average fracture size of the rock can be inferred from the damage in the rock.

4.1.2 TCK damage model

The TCK model was developed based on the G-K model. Taylor et al. (1986) combined the relationship between the Poisson's ratio, the crack density and the effective bulk modulus proposed by Budiansky and O'connell (1976) with the fragment size expression proposed by Grady. According to the model, the dynamic load damage of rock can be divided into two parts: when the rock is in the state of volume compression, the rock belongs to the elastic–plastic material; When the rock is in the state of volume tension, the brittle fracture of rock occurs. The crack density of the rock is expressed as:

$$C_\mathrm{d} = N\alpha^3 \tag{7}$$

where, α is the average radius of crack, expressed as:

$$\alpha = k_1 \cdot \frac{1}{2}\left[\frac{\sqrt{20}K_\mathrm{IC}}{\rho C_\mathrm{P}\varepsilon_\mathrm{max}}\right]^{\frac{2}{3}} \tag{8}$$

where, k_1 is the proportional coefficient; ε_max is the maximum volume strain rate; ρ is the rock density; C_P is the longitudinal wave velocity in the rock, and K_IC is the fracture toughness of the rock.

It can be concluded that:

$$C_\mathrm{d} = \frac{5}{2}km\left[\frac{K_\mathrm{IC}}{\rho C_\mathrm{P}\varepsilon_\mathrm{max}}\right]^2 \varepsilon^{m-1}\varepsilon_x\left(1 - D_x\right) \tag{9}$$

Then the TCK model which can predict the dynamic response of rock under volumetric tensile is obtained as follows:

$$D = 1 - \frac{\overline{K}}{K} = \frac{16}{9}\frac{\left(1-\overline{\mu}\right)}{1-2u}C_\mathrm{d} \tag{10}$$

The relationship between the crack density and the Poisson's ratio can be expressed as:

$$C_\mathrm{d} = \frac{45}{16}\frac{\left(2-\overline{\mu}\right)}{\left(1+\overline{u}\right)\left[10u - \overline{u}(1+3u)\right]} \tag{11}$$

Based on the above two damage models, scholars have conducted more in-depth researches. Suo (2005) analyzed the macro damage law of coal and rock mass during pre-weakening blasting by using the TCK model in the super-dynamic blasting test on the large coal samples. Guo et al. (2023) further improved the dynamic damage model of rock by introducing the cohesion factor and deducing the weakening formula of rock mechanics. Kuszmaul (1987) proposed the KUS model based on the premise that the damage at high density conditions would lead to a decrease in the activation rate of microcracks, combining the isotropic damage model and TCK model of rock blasting. Thorne et al. (1990) considered the influence of the change of rock volume caused by the number of crack activation on the damage change, to enhance the applicability of the KUS model with the high crack density. Huang et al. (2002) based on the dynamic growth and damage evolution of microcracks, studied the dynamic damage evolution of rock under the condition of uniaxial compression, and proposed the corresponding damage constitutive model. By observing the destruction process in coal and rock mass under uniaxial compression using CT scanning, Dai et al. (2004) divided the damage degree of coal and rock mass into four stages, and proposed the distribution function for damage degree at corresponding stages respectively. Zuo et al. (2010) proposed a dynamic damage constitutive model of the brittle materials under the influence of plastic deformation. Zhou and Li (2009), Zhou (2010) proposed a micromechanical model for the damage mechanism of microcracks in brittle rocks under the dynamic loading. Based on this, Yang and Wang (1996) proposed a fractal model of rock blasting damage by means of the fractal theory. Wang et al. (2019) built a dynamic damage constitutive model of coal and rock under the dynamic loading based on the theory of statistical damage and rock mechanical strength.

In the subsequent studies, the damage process of rock mass can be expressed by macro damage variable and micro damage variable respectively. The macro damage variable means that the material can intuitively reflect the damage process at the macro level, which can be calculated by elastic constant, yield stress, tensile strength, elongation, density and acoustic velocity. The reaction damage trend conforms to the macro damage, by which the internal fracture penetration of rock mass can be quantitatively evaluated. The micro damage variable needs to be defined in terms of the damage area and damage unit volume, which can quantitatively evaluate the specific damage value of rock mass, possessing a clear physical significance. The definitions of several commonly used damage variables are shown in Table 4.

Table 4 Definition of damage variables

	Parameters	Equations of damage variables	Note
Macro perspective	Elastic modulus	$D = 1 - \frac{E\prime}{E}$	E' is the elastic modulus of the material with damage; E is the non-destructive elastic modulus
	Elastic modulus	$D = 1 - \left(1 - \frac{\varepsilon^E}{\varepsilon}\right)\frac{E\prime}{E}$	ε^E is the elastic strain; ε is the total strain
	Ultrasonic wave velocity	$D = 1 - \left(\frac{v\prime}{v}\right)^2$	v' is the propagation speed of ultrasonic waves in rock mass under damaged conditions, m/s; v is the propagation speed of ultrasonic waves in rock mass under non-destructive conditions, m/s
	Density	$D = 1 - \frac{\rho\prime}{\rho}$	ρ' is density of damaged rock mass; ρ the density of the non-destructive rock mass
Microscopic perspective	Area of damaged element	$D = \frac{S_D}{S}$	S is the assumed original cross-sectional area of rock mass; S_D the damage area formed by rock under external loads
	Volume of damaged element	$D = \frac{V_D}{V}$	S is the assumed original area of rock mass; S_D is the volume of damaged rock mass under external loads

Gayathri and Srinikethan (2019) proposed to illustrate the damage evolution process of materials from the perspective of macro elastic modulus. The elastic modulus of rock mass will decrease after damage, and the damage degree of coal mass can be reflected through the decrease of elastic modulus. Xie et al. (2005) modified the damage variable defined by Lamaitre's elastic modulus according to its applicable conditions by analyzing from the perspective of energy dissipation and release. The crack defects in rock mass are rather sensitive to the ultrasonic wave. When various sound waves propagate in rock mass, they will interact with rock. When ultrasonic wave passes through rock mass, the characteristics of transmitted wave can show some mechanical information of rock mass. Therefore, the crack defects in rock mass can be better detected by ultrasonic wave. Yang and Gao (2000) and Liu et al. (2009) studied the shock damage characteristics of rock by means of ultrasonic testing. The research showed that the change of acoustic wave velocity could quantitatively characterize the damage evolution degree of rock. The method of defining damage variable by density is basically similar to that of defining elastic modulus. According to the law of mass conservation, the density of rock before and after damage is determined by the means of physical measurement to determine the damage variable. The methods of defining damage variables from the microscopic perspective are directly referred to the original definition methods of damage variables.

Under the impact loading of CSW, the measured damage values of rock mass often change greatly during the damage process because they are hard to be measured directly and accurately by the existing detection methods. Hence, there are some difficulties in the process of practical application. At present, the parameters of damage variables defined from a macroscopic perspective are intuitive, which are widely used with an easy access to the data. However, it is insufficient to describe the damage evolution state of micro cracks in rock mass.

4.2 Damage-stress-seepage coupling model

For the simulation of gas extraction, the evolution of permeability is a key issue in the process of gas extraction in coal seams. Many scholars consider establishing many permeability models under different stress and gas conditions in coal. Gray (1987) proposed a coal permeability model in 1987, which was expressed by the stress method, considering the increase of effective stress caused by the decrease of fluid pressure and the shrinkage of coal matrix caused by gas desorption in the process of coal seam CH_4 production. Seidle and Huitt (1995) considered the effect of shrinkage of the gas desorption from coal matrix, and assumed that all strains were caused by adsorption-induced strains. The permeability evolution model based on porosity change was derived. Gilman and Beckie (2000) proposed a simplified permeability evolution model based on the facts that coal is a relatively regular cleat system, and the mechanism of methane adsorption, desorption and slow migration from matrix to cleat will cause significant changes in permeability. The model relates the permeability of coal with the mean normal stress and expresses the evolution of permeability with the change of stress. Cui and Bustin (2005) quantitatively studied the effects of reservoir pressure and adsorption-induced strain on coal seam permeability based on the adsorption isotherm of coal samples from the Cretaceous Mesaverde Formation, and derived a stress-related permeability model. The above permeability models assume that the coal is in uniaxial compression state with the constantly vertical stress and without the horizontal displacement. The adsorption/desorption of gas and the effective stress of coal are the main

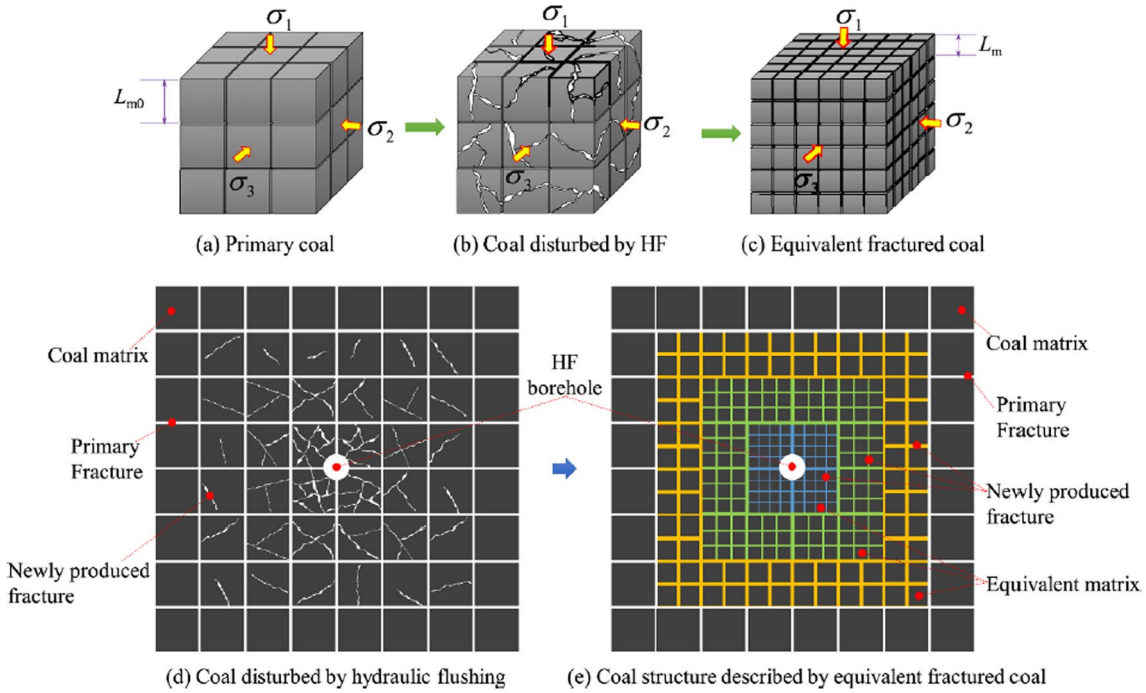

Fig. 14 Schematic diagram of permeability evolution after damage (Liu et al. 2021)

influencing factors, which play a key role in permeability. The above permeability model can be used as the permeability evolution when the coal is not damaged.

Under the disturbance of external forces, such as drilling, mining, blasting and other activities, the coal is subjected to repeated loading and unloading, resulting in the damage and destruction of the coal, the expansion of primary cracks in the coal, and the germination, expansion and penetration of new cracks, as shown in Fig. 14. Due to the expansion of the damaged primary fractures in the coal, the permeability of the coal can be increased hundreds of thousands of times. Based on the Cui&Bustin model, the permeability surge coefficient ζ is introduced to represent the permeability changes caused by damage (Zheng et al. 2017; Fan et al. 2023b).

When the coal seam is subjected to CSW, it will induce the initiation, expansion and penetration of internal micro cracks, resulting in the coal seam being damaged or broken. The damage not only degrades the mechanical properties of coal, but also significantly changes its permeability. In addition, the

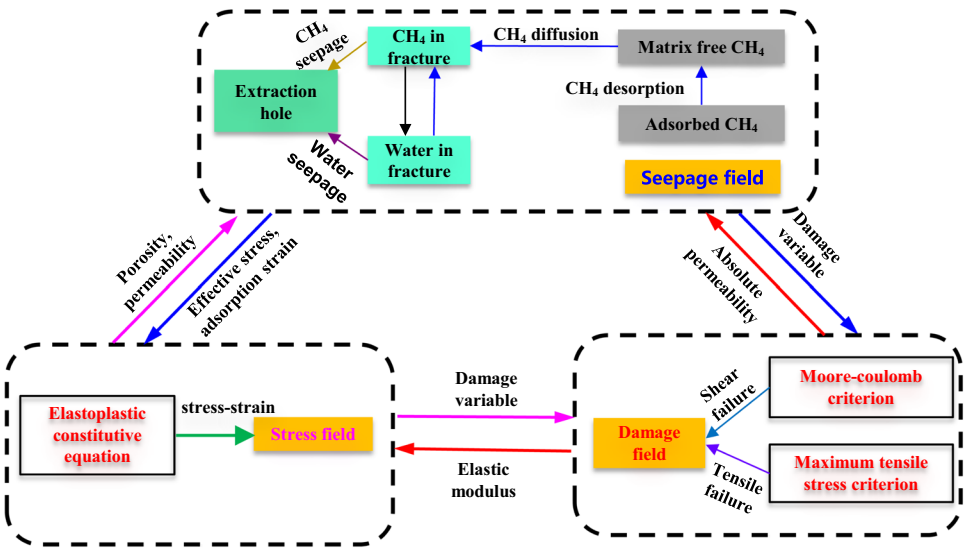

Fig. 15 Coupling relationship in coal between damage and stress seepage

changes of mechanical strength and permeability of coal will affect the seepage of the gas and water in coal, and further affect the distribution of effective stress and pore pressure in coal. On the contrary, the changes of coal stress and pore pressure will lead to the change of effective stress, which will lead to the further development of the internal damage of coal. The interaction and coupling among seepage, stress and damage is called stress-damage-seepage coupling (Fan 2019), as shown in Fig. 15.

For the mathematical model, reasonable assumptions about the complex problem of fracturing coal to enhance gas extraction by CSW are necessary to be made:

The assumptions on the mechanical properties of coal (Rao et al. 2022): (1) The coal is regarded as an elastic–plastic medium with volume force, without considering the heat effect and the gas pressure on the fracturing; (2) The fracture of coal mass under shock wave meets Mohr–Coulomb criterion and maximum tensile stress criterion; (3) The complex physical process acting on a solid is simplified into a stress boundary treatment in which the stress changes with time.

The assumptions on the gas migration related physical properties (Fan et al. 2021a; Luo et al. 2022): (1) Coal is a porous elastic medium including pores and fractures; (2) The gas migration in the matrix is driven by the concentration gradient, which conforms to the Fick diffusion law; and the gas migration in fractures is driven by pressure gradient, which is consistent with the Darcy's law; (3) CH_4 is regarded as an ideal gas, which ignores the gas gravity and takes the gas slippage effect into consideration; (4) Water in coal and rock only exists and migrates in fractures; (5) The adsorption and desorption of CH_4 in coal is completed at constant temperature.

The total strain of coal mass is the sum of the strain caused by the common action of CSW and in-situ stress, the strain caused by pressure of fluid on coal in matrix and fracture, and the strain of coal matrix caused by gas adsorption and desorption. According to the Navier's stress–strain relationship, the control equation of the stress field of coal during the CSW fracturing process is obtained (Xu et al. 2023):

$$Gu_{i,jj} + \frac{G}{1-2\nu}u_{j,ji} = \left(\alpha_m p_{m,i} + \alpha_f p_{f,i}\right) + K\varepsilon_{a,i} \tag{12}$$

Many scholars have studied the initiation and expansion mechanism of coal cracks under impact loading, finding that the origin of coal cracks follows the maximum tensile stress criterion, mainly with the tensile damage. When the stress state meets the maximum tensile failure criterion and the Mohr Coulomb criterion, the coal will produce tensile and shear damage failure (Fan et al. 2023a):

$$\begin{cases} F_1 \equiv \sigma_1 - f_{t0} \\ F_2 \equiv -\sigma_3 + \sigma_1\left[(1+\sin\theta)/(1-\sin\theta)\right] - f_{c0} \end{cases} \tag{13}$$

where θ is the internal friction angle of coal; F_1 and F_2 are damage threshold functions respectively.

The damage variable can be defined as:

$$D = \begin{cases} 0\, F_1 < 0, F_2 < 0 \\ 1-\left|\dfrac{\varepsilon_{t0}}{\varepsilon_t}\right|^n F_1 = 0, \mathrm{d}F_1 > 0 \\ 1-\left|\dfrac{\varepsilon_{c0}}{\varepsilon_c}\right|^n F_2 = 0, \mathrm{d}F_2 > 0 \end{cases} \tag{14}$$

The migration equation of gas in matrix:

$$\frac{\partial}{\partial t}\left(\varphi_m \frac{M_g}{RT}p_a + \rho_c \frac{M_g}{RT}p_a \frac{a_1 b_1 p_{mg}}{1+b_1 p_{mg}}\right) = -\frac{M_g}{\tau RT}\left(p_{mg} - p_{fg}\right) \tag{15}$$

In the fracture, according to the generalized Darcy law of gas–water two-phase flow, the Darcy seepage rates of gas and water are (Yang et al. 2023a):

$$\begin{cases} q_g = -\frac{kk_{rg}}{\mu_g}\left(1+\frac{b}{p_{fg}}\right)\nabla p_{fg} \\ q_w = -\frac{kk_{rw}}{\mu_w}\nabla p_{fw} \end{cases} \tag{16}$$

where, b is the Klinkenberg factor, PA; μ_g is the dynamic viscosity of gas CH_4, Pa·s; μ_w is the dynamic viscosity of water, Pa·s.

In a unit volume of coal, the change of free gas in the crack is equal to the sum of the gas seeping out (into) the crack and the gas diffusing into (out) the crack. As for gas, it first desorbs from the matrix pore surface to the pore space, then diffuses from the pore space to the fracture space, and finally seepages from the fracture space to the drainage borehole. According to the conservation of mass, the governing equation of gas migration in the fracture is as following:

$$\begin{aligned} &(s_g\varphi_f \frac{M_g}{RT}p_{fg}) - \nabla\cdot\left(\frac{M_g}{RT}\frac{kk_{rg}\left(p_{fg}+b\right)}{\mu_g}\nabla p_{fg}\right) \\ &= \left(1-\varphi_f\right)\frac{M_g}{\tau RT}\left(p_{mg}-p_{fg}\right) \end{aligned} \tag{17}$$

The seepage governing equation of water in fracture:

$$\frac{\partial\left(s_w\varphi_f\rho_w\right)}{\partial t} - \nabla\cdot\left(\frac{\rho_w kk_{rw}}{\mu_w}\nabla p_{fw}\right) = 0 \tag{18}$$

The damage-stress-seepage coupling model of gas extraction strengthened by controlled shock wave cracking coal was established, considering the coupling relationship between the damage law of coal under shock wave action, the influence of damage in coal seam on permeability, the change of pore structure of coal fissure, the process of gas adsorption and desorption, and the law of gas migration in coal matrix and fracture. It can theoretically describe the

whole process of gas extraction from cracked coal by controlled shock wave. Permeability isotropy is considered in the establishment of permeability models. In reality, the anisotropy of bedding, mechanical properties and stress state of coal seam results in anisotropy of coal permeability.

In these models, reasonable assumptions are made on the coal seam to simplify the calculation steps, and mathematical theories are used to establish corresponding mathematical models. In order to calibrate the models and be consistent with the experimental results, the same initial values and boundary conditions should be set according to the experimental conditions, and the required parameters in the models can be accurately measured.

5 Research advances in field test of CSW fracturing enhanced gas extraction

5.1 Equipment and technology of CSW fracturing enhanced gas extraction

The controllability of CSW fracturing enhancement permeability technology mainly refers to that the impact effect and the engineering operation area are controllable. The amplitude of shock wave can be effectively controlled by compounding energetic materials of different qualities and types with metal wires. The quality and types of energetic materials can be reasonably controlled according to the fracture strength of coal and the collapse strength of hole wall, so as to realize the controllable pressure and duration of shock wave. By means of mobile equipment, multi-point balanced impact is carried out inside the borehole to achieve the operation area being controllable and reach the purpose of stimulating the whole hole end and reforming the coal seam.

For the underground implementation equipment of CSW fracturing, the CSW fracturing device was developed and was successfully applied to the practice of coal permeability enhancement. As shown in Fig. 16, the device includes the shock wave generator in the hole and the pulse power controller outside the hole. The shock wave generator inside the borehole is the main core, including pulse power controller, high voltage DC power supply, energy storage capacitor, energy controller and energy converter. In order to implement the CSW fracturing, the high-voltage DC power supply, energy storage capacitor, energy controller and energy converter are integrated into a cylindrical rigid unit with an outer diameter of 90 mm. The out-of-hole unit is a small pulse power controller, which is used to send work orders to the device inside the hole, receive the feedback of the working status of the hole entry device and display the information on the human–computer interaction panel (Li et al. 2023).

The working principle of the CSW fracturing field equipment is as follows:

(1) The out-of-hole pulse power controller establishes a signal channel through the central cable drill pipe with the drilling equipment, and sends orders to the device inside the borehole to control the operation of the device in the borehole;
(2) When the device inside the borehole receives the order signal from the pulse power controller, the high-voltage DC battery pack starts to charge the energy storage device. When the energy storage device reaches

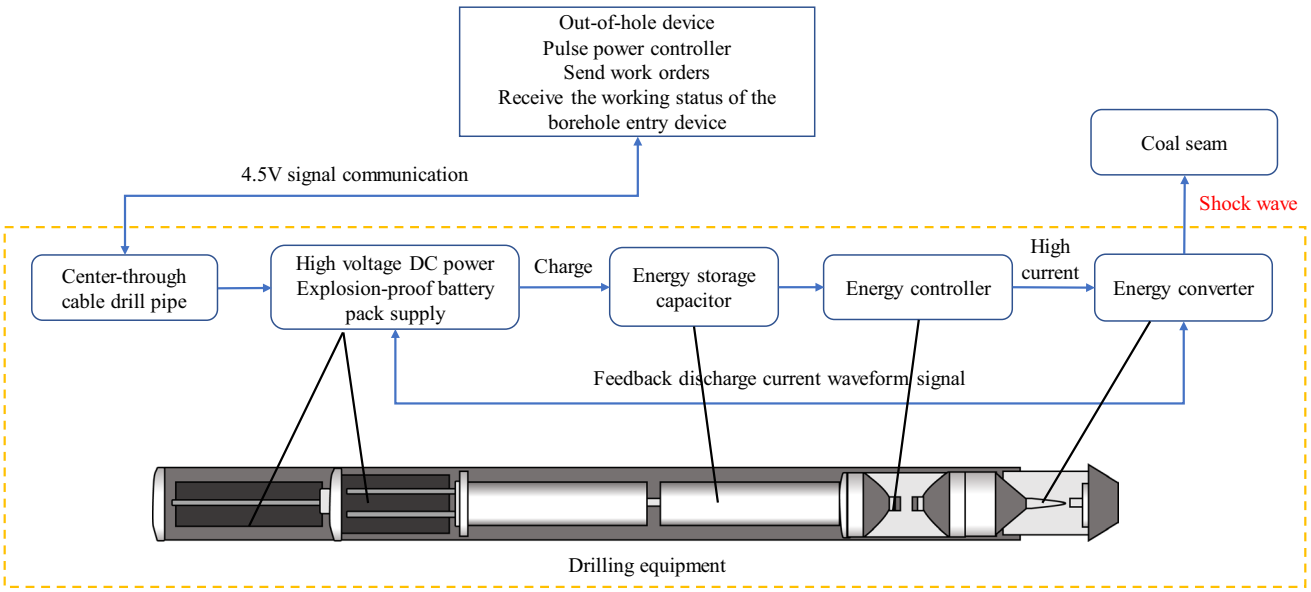

Fig. 16 Working principle diagram of field equipment of CSW fracturing (Li et al. 2023)

the preset threshold of the energy controller, the stored electric energy is transferred to the energy converter through the energy controller;

(3) In the energy converter, the current is applied to make the metal wire rapidly vaporize and ionize, exciting the energetic material, and coupling them with the water medium in the borehole, which can convert the electrical energy and chemical energy of energetic material into mechanical energy—the pulse shock wave, and then acting on the coal seam.

In the field implementation, the operation process of CSW fracturing enhanced permeability of coal seam is as follows: First, push the shock wave generator equipment to the target coal seam section by the drilling rig and drill pipe. Then seal the orifice and inject clean water into the hole. Followed that, divide the whole borehole into several operation sections, and carry out multiple shock wave operations for each section from the bottom of the borehole, as shown in Figs. 17 and 18. After that, the shock wave generator is then pushed back by the rig to the next operation section and the operations are carried out sequentially. In order to solve the problem that the borehole wall in soft coal seam is easy to collapse, it is necessary to support the borehole wall with glass fiber reinforced plastic screen before installing the CSW generator to enhance the coal permeability.

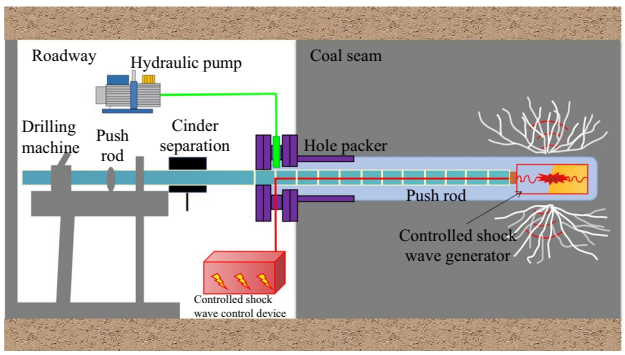

Fig. 17 Sketch of site operation in underground coal mine

5.2 Cases of field application

Scholars proposed to apply the CSW induced by high-voltage pulse combined with metal wire and energetic materials to coalbed methane (CBM) extraction. The instantaneous loading effect of shock wave generated by high-voltage discharge is used to change the CBM occurrence state and increase reservoir fractures, so as to improve the reservoir permeability and enhance the CBM extraction efficiency. Relevant field tests have been carried out in a several coal mines in China, as listed in Table 5. The field tests mainly study the construction parameters and effective radius of the CSW in the borehole, which makes up for the deficiency of the small-scale experiment in the laboratory.

5.2.1 Huangling coal mine

The field test is located in the gas abnormal area in the return airway of 209 panel in Huangling No. 2 coal mine. The operation of CSW fracturing is mainly carried out in five boreholes. The specific operation parameters and main results are shown in Table 6. The parameters include the operating point spacing (10, 9.5 and 7 m) and operation times of single point (5 and 8 times).

Fig. 18 Picture of CSW fracturing in situ of underground coal mine

Table 5 Statistics of field pilots of CSW fracturing in coal mine, China

Experimental location	Gas content of coal (m^3/t)	Permeability coefficient (m^2/MPa^2 d)	Firmness coefficient of coal seam	Effect of permeability enhancement
Huangling coal mine	6.59–7.17	0.00832	2.3	The natural gas emission from enhanced permeability boreholes is 1.36–2.42 times that of conventional boreholes, with an average of 1.97 times that of conventional boreholes. The pure gas extraction from boreholes is 3.67–7.54 times that of conventional boreholes, with an average of 5.096 times
Jining coal mine	8.23	0.0230–0.0858	0.6	The average daily extraction volume of soft coal drilling increased by 5–5.9 times
Linhua coal mine	23.42	0.05–7.17	0.35–1.7	The gas volume for CSW enhanced boreholes and observed boreholes has increased by 2.5 times and 2 times respectively compared to conventional boreholes
Baode coal mine	–	0.17–0.8	0.72	Under the action of repetitive compression waves, the gas flow rate in observation holes 1 and 2 near the test hole significantly increases and shows a decreasing trend over time
Zhongjing coal mine	11	0.1115	0.34	After the CSW fracturing, the average daily gas extraction amount of a single hole increased by 3.37 times, reaching a maximum of 6.54 times. The average gas concentration has increased by 2.31 times, and the effective radius of enhanced permeability has reached 40-60 m
Yanchuan south coal reservoir	12	–	–	The initial gas production has increased significantly, and some wells can last for more than 6 months

By analyzing the test data of each borehole, it can be concluded that the permeability enhancement effect of the operating point spacing of 10 m is better than that of 7.5 m under the same impact operating times. Under the same operating spacing, the permeability enhancement effect of 8 times of impacts on a single point is better than that of 5 times. In terms of impact density, the greater the impact density is, the more obvious the permeability enhancement effect is (Yan et al. 2021).

5.2.2 Jining coal mine

Jining Coal Mine, located in the southwest of Hedong Coalfield, is a high gassy mine with a single thick coal seam. The extraction radius of conventional borehole is 2 m, and the standard extraction time is about 90 days. There are three groups of boreholes designed to test the permeability enhancement effect of CSW fracturing: the first group equipped with three boreholes with CSW fracturing enhanced coal permeability, and a certain number of inspection boreholes were arranged around them. The effective radius of CSW fracturing enhancement can be analyzed by the extracted gas volume of the inspection boreholes. The second group is arranged with two boreholes with CSW fracturing enhanced coal permeability, without inspection boreholes around them. The impact operations are carried out in a single point of 5 times and a single point of 6 times respectively, to investigate the extraction effect of different impact operation times. The third group was designed with two boreholes with CSW fracturing enhanced coal permeability with a spacing of 40 m to investigates the extraction effect. The field layout of the three groups of pilots is shown in Fig. 19 (Wang et al. 2019; Su 2020).

Figure 20a shows the relationship between the spacing of the inspection boreholes and the increase times of extracted gas volume in the first group of pilots. The peak value of the gas volume occurs at 10 m away from the impact borehole, and the increment of the gas extraction content can appear at 40 m. However, considering that the gas content of the coal seam must reach the standard within a certain extraction time, the effective radius of the test is ultimately considered to be 17 m. Figure 20b shows the results of the second group of pilots. The average gas volume of No. 3 borehole with 5 impacts at single point is lower than that of No. 5 borehole with 6 impacts at single point. With the increase of impact times, the overall gas volume of borehole is on the rise. The test results of the third group, in Fig. 20c, show that the two changes in the extraction volume of adjacent boreholes can be roughly divided into a negative correlation stage and a stable stage. Before 60 days of extraction, the negative pressure of extraction was not transmitted in a timely manner, and the impact effect led to the conduction of cracks between the two boreholes, resulting a negative correlation between the extracted gas volume of two boreholes and the occurrence of negative pressure. With the increase of the extraction time, the negative pressure is gradually balanced

Table 6 Construction borehole parameter

Number of boreholes	Depth of borehole (m)	Point spacing (m)	Operating times of single point	Monitoring time (d)	Natural gas emission volume (m^3/min hm)	Extract pure quantity (m^3/min)	Extraction concentration (%)
S1	174	10	5	75	0.0306	0.2486	47
S2	150	9	8	85	0.0452	0.2287	60.62
S3	162	7.5	8	61	0.0276	0.2702	60.63
S4	150	7.5	8	58	0.0242	0.47	62
S5	153	7.5	5	59	0.0188	0.37	41.04
S6	–	–	–	38	0.0109	0.0623	24.13

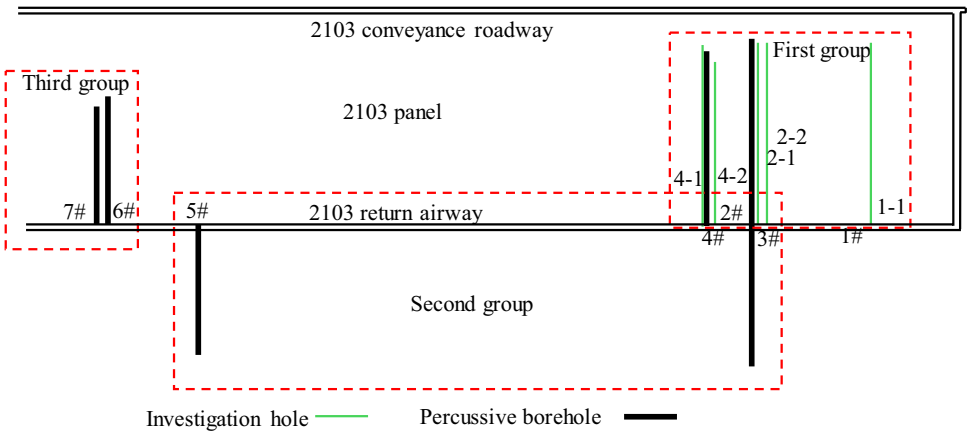

Fig. 19 Drilling layout of CSW fracturing enhanced coal permeability (Wang et al. 2019)

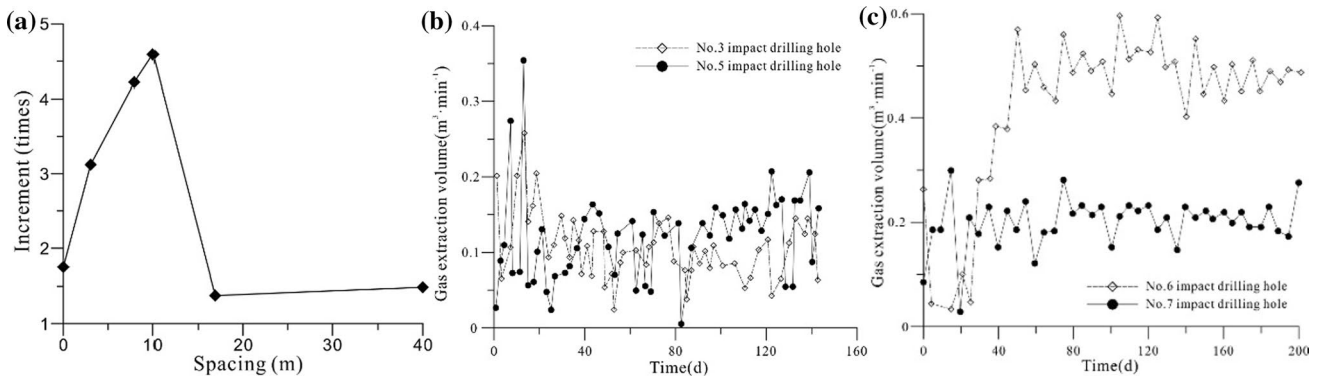

Fig. 20 Results of CSW fracturing test in Jining Coal Mine (Su 2020)

to all parts of the coal. The gas desorption in the coal seam is significantly accelerated. With the increase of the flow rate, the gas extraction will offset the "negative pressure" and finally present a stable high-yield state.

5.2.3 Linhua coal mine

Linhua coal mine, located in Jinsha County, Guizhou Province, is a coal and gas outburst prone mine, which mainly mining seam is the No. 9 coal of Permian Longtan Formation. There were two field tests carried out in this area. The first designed one in-seam borehole as a CSW fracturing borehole, and seven observation boreholes were set around the CSW fracturing borehole. An impact point is set every 9 m in the CSW fracturing borehole with a single point of 8 impacts. According to the statistics, the gas extraction purity of the 100-m borehole by CSW fracturing is 2.5 times that of the conventional borehole. The gas extraction purity of the 100-m borehole with observation hole in the CSW fracturing area is 2.0 times that of the conventional borehole, which

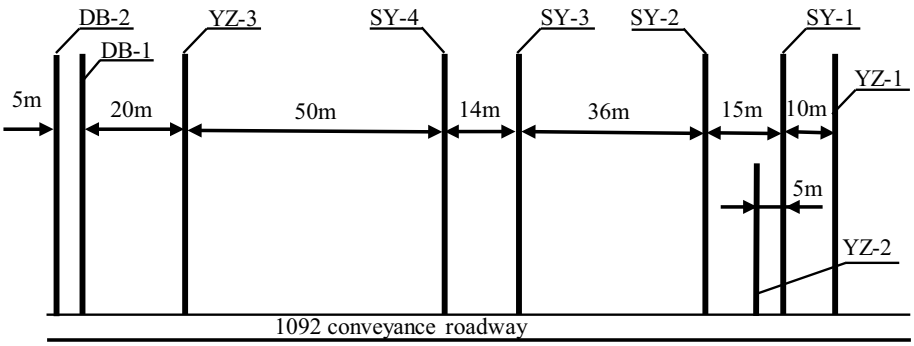

Fig. 21 Borehole layout of CSW fracturing enhanced coal permeability in the second test in Linhua Coal Mine (Li et al. 2019a)

Table 7 Construction borehole parameters and results of CSW fracturing in Linhua Coal Mine (Li et al. 2019a)

Number of boreholes	Diameter of borehole (mm)	Distance between shock boreholes (m)	Number of single shock borehole (times)	Range of single shock borehole (m)	Average pure gas volume of single shock borehole (m^3/min)	Accumulated pure gas volume (m^3)	Average concentration of single shock borehole (%)
SY-1	113	6	5	30	0.094	13,751.28	23.7
SY-2	113	6	3	54	0.104	14,695.92	54.0
SY-3	113	9	3	54	0.108	15,089.76	49.6
SY-4	113	6	3	30	0.115	15,266.88	52.3
DB-1	113	–	–	–	0.052	1046.16	5.7
DB-2	113	–	–	–	0.036	731.52	2.7

verifies the effectiveness of CSW fracturing in this coal mine (Li et al. 2019a).

Figure 21 shows the borehole layout of the second test, in which the SY-1-SY-4 is an anti-reflection hole of CSW, the YZ-1-YZ-3 being the drill hole to verify the change of gas content in the test area, and the DB-1 and DB-2 are the ordinary boreholes 70 m outside the test area to compare the gas extraction effect. The extraction data of the drilling are shown in Table 7.

According to the extracted gas volume of the CSW fracturing borehole and the observing borehole, the average gas concentration of the CSW fracturing borehole is 44.7% with an average purity of 0.105 m^3/min, which are 1.08 times and 9.64 times higher than that of conventional borehole respectively. The gas content of coal seam in the original area of 1092 conveyance roadway was about 11.15m^3/t. After 100 days of extraction tin CSW fracturing borehole, the gas content decreased to 4.38 m^3/t and 5.31m^3/t, and the pre-extraction rate of gas is more than 50%, with a good extraction effect (Zhang et al. 2023b).

5.2.4 Zhongjing coal mine

Zhongjing coal mine is located in Liupanshui city, Guizhou Province, China. The coal seam K9 is the target layer for CSW fracturing operation. The working area is 10,903 Panel, with a buried depth of 200 m, a strike length of 806 m, a dip length of ~ 200 m. The thickness of coal seam is 0.56–3.44 m with an average of 2.23 m. The structure of coal seam is crushed mylonite coal, and the firmness coefficient is only 0.34, belonging to extremely soft coal seam. The average gas content is 10.99m^3/t, and the permeability coefficient is 0.1115 m^2/MPa^2 d. There are two types of extraction boreholes designed: the first one is drilled head-on the excavation working face. The 16#, 17#, 18# boreholes from the conveyance roadway and the 15# borehole from the return airway are used for gas extraction of non-mining wall. The second type is drilled on the coal mining wall. The borehole spacing is set as 40 m for the 8 permeability enhancement boreholes, 6 ordinary boreholes and 2 auxiliary extraction boreholes. The ordinary boreholes are used to study the effectual gas extraction distance, and the auxiliary extraction boreholes play a protective role in the drilling. The drilling layout is shown in Fig. 22. The statistics of field implementation of gas extraction are shown in Table 8.

The results show that the average daily gas extraction of the 12 CSW fracturing boreholes is 994m^3/d, and the average daily gas extraction of the 6 ordinary boreholes is 295 m^3/d. Through comparative analysis of the extraction volume of boreholes 3#, 4# and 5# in the return airway, the effective radius of the permeability enhancement of coal seam by CSW is about 40–60 m. After the antireflection operation, the effect of the first type of antireflection holes is generally better than that of the second type of antireflection holes. It is speculated that the non-drilled antireflection holes are not affected by the mining of the working face. The

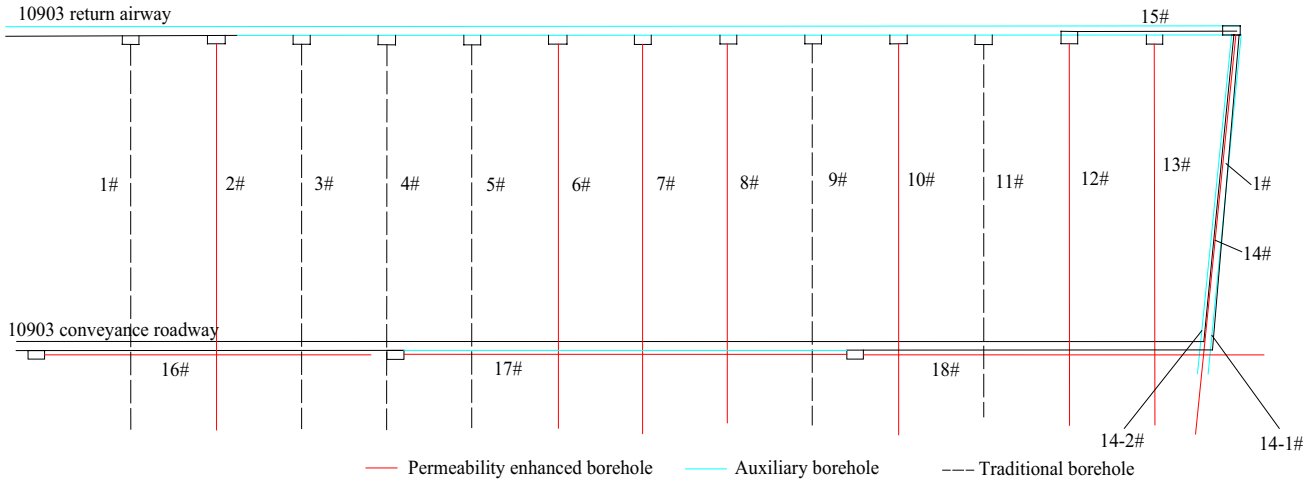

Fig. 22 Borehole layout for CSW fracturing enhanced gas extraction in Zhongjing coal mine (Zhang et al. 2017b)

Table 8 Statistics of the CSW fracturing field test on 10,903 working face in Zhongjing coal mine

Boreholes	Actual drilling length (m)	Length of permeability enhanced section (m)	Number of shock	Density of shock (times/m)	Daily average gas extraction pure volume (m^3)
16#	190	150–30	119	0.99	2985
17#	260	220–25	320	1.64	528
18#	260	220–25	320	1.64	1065
2#	198	144–29	121	1.05	489
6#	213	140–25	128	1.11	363
7#	213	90–25	70	1.08	919
8#	210.5	95–25	75	1.07	822
10#	225	97–25	72	1.03	704
12#	207	155–25	130	1.00	667
13#	205.5	150–25	125	1.00	626
14#	222	200–25	175	1.00	2400
15#	93	90–25	70	1.08	364
1#	214	–	–	–	141
3#	201	–	–	–	365
4#	214	–	–	–	186
5#	216	–	–	–	234
9#	210	–	–	–	464
11#	211.5	–	–	–	377
14–1#	228	–	–	–	353
14–2 #	205.5	–	–	–	351

gas extraction effect of 15# boreholes in the transport lane with impact density of 0.99 times/m is significantly better than that of 17# and 22# boreholes in the transport lane with impact density of 1.64 times/m, which shows that the times of impact action of CSW is not the more the better. With the more times of impacts, the permeability enhancement effect of coal seam will be limited by the pulverized coal fragmentation. It is necessary to consider the reasonable impact density for the specific coal strength in the on-site practice (Zhang et al. 2019c).

5.2.5 Baode coal mine

The 8 # coal seam of Shanxi Formation, as the main coal seam of Baode Coal Mine, is characterized by low permeability, large attenuation coefficient of borehole, and development of cracks in coal wall. There are also some problems

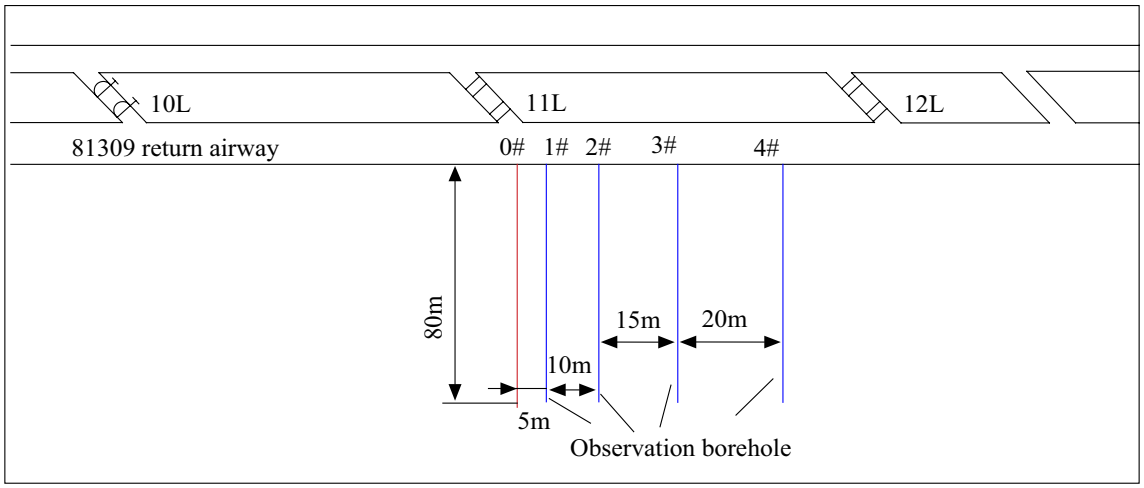

Fig. 23 Borehole layout for CSW fracturing enhanced gas extraction in Baode coal mine (Zhang et al. 2019a, b, c, d)

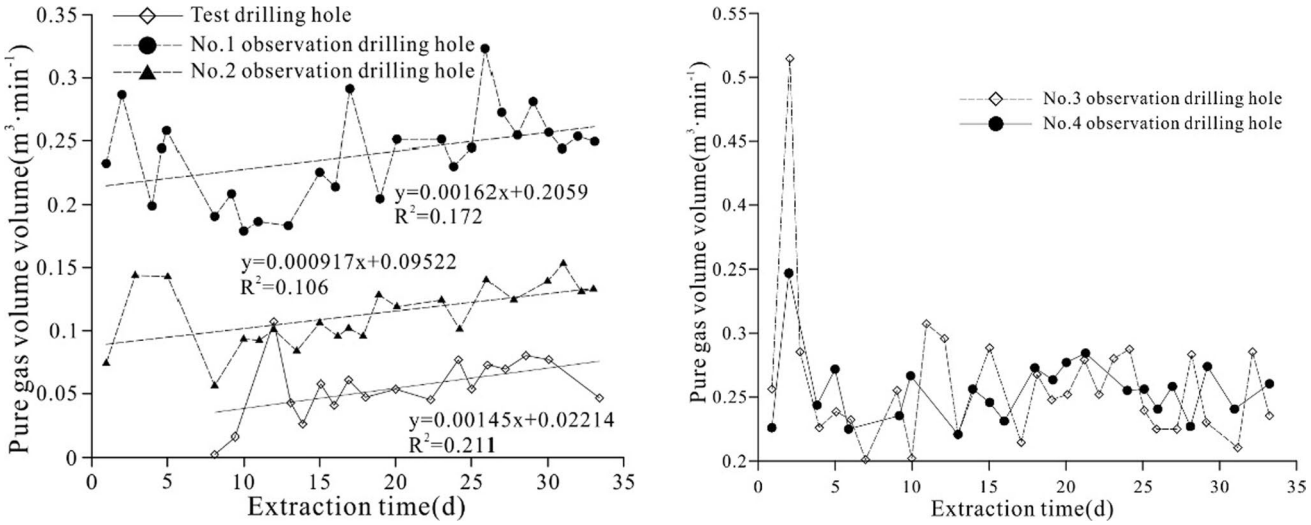

Fig. 24 Results of CSW test in Baode coal mine (Zhang et al. 2019b)

such as low gas extraction rate, long pre-extraction time, and difficult gas control at the working face. Firstly, a pilot test was conducted at Baode Coal Mine, where the permeability enhancement operation in the coal seam with a length of 10 m in the whole 30–40 m test hole. Considering the process parameters of shock wave permeability enhancement operation in the surface coalbed methane and oil wells, it was set that starting from a hole depth of 40 m, there was one operating point every 2 m, with 15 impacts on each operation point, and a total of 30 impacts on the 30 m operation point. There were a total of 5 parallel boreholes with a depth of 80 m arranged, with 1 borehole for enhanced permeability and 4 boreholes for observation, in which the four observation boreholes were located 5 m, 15 m, 30 m, and 50 m away from the enhanced permeability borehole the effective range of CSW fracturing is studied. The borehole layout is shown in Fig. 23.

As shown in Fig. 24, the experimental borehole with CSW fracturing has the lowest purity during the gas extraction. The high impact density leads to the destruction of the coal seam inside the enhanced permeability borehole and inhibits the effect of gas extraction. For boreholes 1# and 2# in the near field, the purity of gas extraction has increased significantly and continuously. Compared with boreholes 3# and 4# in the far field, the purity of gas extraction has increased in the early stage of extraction without increasing trend.

In the second group of test, there is a more detailed test conducted on the basis of the pilot test, which added the number of test groups, with the distance of 80 m between each group. The influence of superimposed anti-reflection

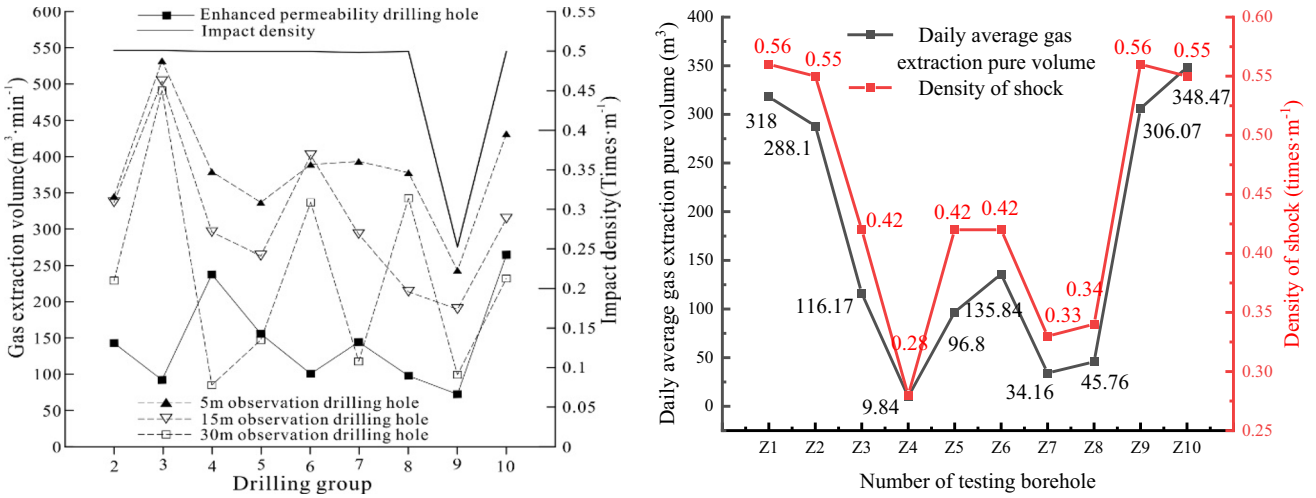

Fig. 25 Results of CSW fracturing test in Baode coal mine (An et al. 2020)

effect between the two groups of tests was eliminated, as well as the influence of different impact densities on the antireflection effect of controllable shock waves was analyzed. Figure 25 is a comparison chart of gas extraction results in the boreholes, which shows that within the range of 100 m permeability enhancement in the borehole, the impact density of 0.5 times /m has the best operation effect. When the radius of permeability enhancement effect by CSW is above 30 m, the permeability enhancement effect gradually becomes worse and worse with the increase of distance. Then, the impact antireflection effect was carried out on 10 boreholes, and four impact density parameters (0.5, 0.4, 0.3, 0.2 times/m) were designed to verify the influence of different impact density on the antireflection effect by CSW, finding that within the range of 100 m permeability enhancement in the borehole, the impact density of 0.5 times /m has the best operation effect (An et al. 2020).

5.2.6 Southern Yanchuan coalbed methane field

This test area is located in the southern section of the Ordos Basin, and the No. 2 coal in Shanxi Formation is mined with an average coal thickness of 5 m, in which the gas content of the coal seam is generally high with an average of 12 m^3/t. The coal is characterized by relatively developed microcracks, low mechanical strength and easy fracture. There are common problems of the blockage of pulverized coal and the decline of gas production.

The results show that the application of controllable shock wave plugging removal and permeability improvement technology in coalbed methane wells can improve liquid fluidity, promote gas desorption and diffusion, and remove plugging in coal reservoirs. The well selection criteria of this technology are low coalbed fracture pressure, good fracturing effect, including dirt band, high gas-bearing capacity of coalbed, relatively high formation pressure coefficient, etc. This technology has the effect of creating fractures and removing plugs, which can improve the fluidity of formation fluids and remove formation pollution. It has a good implementation effect and application prospect in the near-well zone of south Yanchuan coalbed methane wells to plugging removal and increase gas production, and is expected to be a new stimulation technology for low yield and efficiency wells (Wang 2020).

6 Future research direction

6.1 Basic principle in coal seam after CSW fracturing

(1) The morphology and expansion characteristics of plasma are not easy to be detected due to the short acting time. New monitoring means are needed to observe the expansion characteristics of plasma channel to facilitate the understanding of the formation mechanism and influencing factors of CSW under different conditions.
(2) Excitation of the chemical energy of energetic materials can improve the intensity of shock wave under the same stored energy. Currently, there are few types of energetic materials. By improving the combination of metal wire and energetic materials and developing new types of energetic materials, the application of CSW can be further improved and engineering costs can be reduced.

6.2 Experiments of coal seam CSW fracturing

(1) In laboratory experiments, the size effect of coal samples will seriously affect the accuracy of experimental results, so it is necessary to improve the experimental standards under different experimental conditions of different sizes, which is conducive to the standardized description of experimental results of controllable shock waves.
(2) In the state of primary rock stress, the crack development of coal body under the influence of CSW is more complicated. In order to better understand the cracking law of coal body under primary rock stress, it is necessary to simulate the stress of primary rock through the true triaxial stress loading system.

6.3 Model of enhanced gas extraction by CSW fracturing

(1) The CSW is often accompanied by heat release when it is excited, and the temperature rise will also lead to changes in the law of gas desorption in coal seams. The coupling model of multiple physical fields of coal stress, temperature, damage and seepage under the action of CSW is improved, so that the simulation results are closer to the real situation on site.
(2) There exist the soft and hard coal variation zones, coal seam thickness variation zone, magma intrusion, fold tectonic zone, fault tectonic zone, and other natural geological structure abnormal areas in the coal seam. The existence of geological anomalies will change the strength of coal and greatly affect the damage evolution of coal and gas migration law. Relevant numerical simulation research on CSW under complex geological conditions will be conducted in future works.

6.4 Field test of CSW fracturing enhanced gas extraction

(1) At present, the CSW reflection range is determined mainly through the gas extraction situation of the observation hole around the drilling hole, the internal stress monitoring means of coal seam is updated, the propagation attenuation law of shock wave intensity and coal seam physical and mechanical parameters on the shock wave in the coal seam is analyzed, and the effective range of shock wave reflection in the coal seam is studied, providing a basis for the construction parameter design in the field application.
(2) Under some special geological conditions, CSW technology is combined with other coal seam permeability enhancing means to control coal seam gas.

7 Conclusions

In this review, it summarizes the research advances on enhanced gas extraction of coal seam by CSW from the perspectives of theoretical analysis, laboratory test, mathematical model and field test. The generation mechanism of CSW and the enhancing framework of coal permeability by CSW fracturing. Equipment development and experimental test on coal seam by CSW fracturing under different factors. The damage-stress-seepage coupling mathematic model. Technical development of coal permeability enhancement by CSW fracturing, and field tests conducted in China. The following conclusions can be drawn:

(1) Based on the different media between electrodes, the CSW can be divided into three categories: hydraulic effect, wire explosion and excitation of energetic materials by detonating wire. During the process of propagation and attenuation of the high-energy shock wave in coal, the shock wave and bubble pulsation work together to produce an enhanced permeability effect on the coal seam. The repeated application of CSW will further cause the fatigue effect on the mechanical properties of coal reservoir.
(2) The coal seam is damaged when the shock wave intensity exceeds the threshold value, and there is an optimal range of the impact of CSW energy on the fracturing effect. Overloading will damage the coal reservoir structure, and the pulverized coal will increase the wave impedance and attenuation in the process of shock wave propagation, reducing the effect of fracturing and permeability enhancement. When underloaded, the higher the shock wave energy is, the more cracks in coal is, and with the greater of length, width and area of cracks. The accumulation of coal damage is proportional to the number of shocks. Under the condition of in-situ stress, the propagation of crack caused by shock wave is restrained, and the crack generated by shock wave preferentially expands along the direction of maximum principal stress.
(3) Gas extraction after CSW fracturing involves a damage-fluid–solid coupling process, and the following factors need to be considered: the structure of fracture and pore in coal, flow of fluid in fracture, diffusion in coal matrix, changes in reservoir stress caused by the migration and desorption of CH_4, effects of damage in coal seam on permeability, and effects of water in coal seam on gas migration in fracture.
(4) The permeability enhancement effect of CSW is affected by the breakage degree of coal seam. The shock wave is absorbed by the broken coal, which may hinder the propagation of CSW, resulting in a poor

effect of permeability enhancement. When arranging two adjacent boreholes for CSW permeability enhancement test, the spacing of boreholes should not be too close, which may lead to negative pressure mutual pulling in the early stage of drainage. At present, the accurate method for effectively predicting the CSW permeability enhanced range should be further investigated.

Acknowledgements This research was financially supported by the National Natural Science Foundation of China (52004117, 52174117 and 52074146), the Postdoctoral Science Foundation of China (2021T140290 and 2020M680975), the Basic scientific research project of Liaoning Provincial Department of Education (JYTZD2023073).

Author contributions CF and HS: Conceptualization, Methodology, Writing—original draft; SL: Methodology, Supervision; LY: Formal analysis; BX and ZY: Writing—review & editing; ML: Visualization; XJ: Writing— review & editing; LW and LZ: Revision.

Declarations

Conflict of interest The authors declare that they have no known competing financial interests.

Open Access This article is licensed under a Creative Commons Attribution 4.0 International License, which permits use, sharing, adaptation, distribution and reproduction in any medium or format, as long as you give appropriate credit to the original author(s) and the source, provide a link to the Creative Commons licence, and indicate if changes were made. The images or other third party material in this article are included in the article's Creative Commons licence, unless indicated otherwise in a credit line to the material. If material is not included in the article's Creative Commons licence and your intended use is not permitted by statutory regulation or exceeds the permitted use, you will need to obtain permission directly from the copyright holder. To view a copy of this licence, visit http://creativecommons.org/licenses/by/4.0/.

References

An S, Chen D, Zhsng Y et al (2020) Application of controllable electric pulse wave antireflection technology in low permeability coal seam. Coal Geol Explor 48(04):138–145

Bao X, Guo J, Liu Y et al (2021) Damage characteristics and laws of micro-crack of underwater electric pulse fracturing coal-rock mass. Theor Appl Fract Mec 111:102853

Barbashova GA, Shomko VV (2007) The discharge mode influence on the hydrodynamic processes of underwater electric explosions. Surf Eng Appl Elect 43:465–469

Bian D (2018) Study on the characteristics of pulse discharge shock wave under hydrostatic pressure and its rock mass fracturing. Taiyuan University of Technology, Taiyuan

Budiansky B, O'connell RJ (1976) Elastic moduli of a cracked solid. Int J Solids Struct 12(2):81–97

Chao Y, Han R, Li X et al (2014) Zero-dimensional simulation of discharge channel properties during underwater electrical wire explosion. High Voltage Eng 40(10):3112–3118

Chen M, Lu W, Zhou C et al (2009) Influence of initial in-situ stress on blasting-induced cracking zone in tunnel excavation. Rock Soil Mech 30(08):2254–2258

Chen W, Maurel O, Reess T et al (2012) Experimental study on an alternative oil stimulation technique for tight gas reservoirs based on dynamic shock waves generated by pulsed arc electrohydraulic discharges. J Petrol Sci Eng 88:67–74

Chen W, Yu Y, Zhang Z (2013) Research on high voltage nanosecond pulse measurement system based on optical fiber transmission technology. Sci Technol Eng 17:4936–4940

Chen B, Barboza BR, Sun Y et al (2021a) A review of hydraulic fracturing simulation. Arch Comput Method 29:1–58

Chen Y, Chu T, Chen X et al (2021b) Comparative analysis of gas–solid–liquid coupling behavior in front of the working face before and after water injection during coal mining. Nat Resour Res 30:1561–1575

Cook JA, Gleeson AM, Roberts RM et al (1997) A spark-generated bubble model with semi-empirical mass transport. J Acoust Soc Am 101(4):1908–1920

Cui X, Bustin RM (2005) Volumetric strain associated with methane desorption and its impact on coalbed gas production from deep coal seams. Aapg Bull 89(9):1181–1202

Dai G, Yin G, Pi W (2004) Research on damage constitutive model and evolution equation of coal under uniaxial compression. J Tongji Univ (natu Sci) 32(8):986–9890

Dougill J W, et al (1976) Mechanics in engineering. ASCE·EMD 333–355

Efimov S, Gilburd L, Fedotov-Gefen A et al (2012) Aluminum microparticles combustion ignited by underwater electrical wire explosion. Shock Waves 22:207–214

Fan S, Zhang D, Wen H et al (2021a) Enhancing coalbed methane recovery with liquid CO_2 fracturing in underground coal mine: from experiment to field application. Fuel 290:119793

Fan C, Yang L, Wang G, et al (2021b) Investigation on coal skeleton deformation in CO_2 injection enhanced CH_4 drainage from underground coal seam. Front Earth Sc-Switz 766011

Fan C, Xu L, Elsworth D et al (2023a) Spatial-temporal evolution and countermeasures for coal and gas outbursts represented as a dynamic system. Rock Mech Rock Eng 56:6855–6877

Fan C, Yang L, Sun H et al (2023b) Recent advances and perspectives of CO_2-enhanced coalbed methane experimental, modeling, and technological development. Energ Fuel 37(5):3371–3412

Fan C (2019) Study on inoculation and evolution law of geological dynamic system of coal and gas outburst. Liaoning Technical University

Feng YJ, Kang H (2012) Test on hard and stable roof control by means of directional hydraulic fracturing in coal mine. Chinese Journal of Rock Mech Eng 31(6):1148–1155

Fu R, Sun Y, Fan A et al (2016) Experimental study on fracturing of high voltage electric pulse in shale gas exploitation. High Power Laser Part Beams 28(07):192–196

Gao B, Zhang H, Zhang C (2003) Experimental study on high-voltage discharge bubbles in water. Acta Phys Sin-Ch Ed 07:1714–1719

Gayathri G, Srinikethan G (2019) Bacterial cellulose production by K. saccharivorans BC1 strain using crude distillery effluent as cheap and cost effective nutrient medium. Int J Biol Macromol 138:950–957

Gilman A, Beckie R (2000) Flow of coal-bed methane to a gallery. Transport Porous Med 41:1–16

Grady DE, Kipp ME (1980) Continuum modelling of explosive fracture in oil shale. Int J Rock Mech Min Sci Geomech Abst 17(3):147–157

Gray I (1987) Reservoir engineering in coal seams: part 1—The physical process of gas storage and movement in coal seams. SPE Reserv Eng 2(01):28–34

Grinenko A, Sayapin A, Gurovich VT et al (2005) Underwater electrical explosion of a Cu wire. J Appl Phys 97(2):023303

Grinenko A, Efimov S, Fedotov A, et al (2006) Efficiency of the shock wave generation caused by underwater electrical wire explosion. J Appl Phys 100(11)

Guo J, Li X, Lu C et al (2023) Modified model and simulation verification of rock-fatigue damage considering repeated discharge impact. Processes 11(8):2366

Han R, Zhou H, Liu Q et al (2015) Generation of electrohydraulic shock waves by plasma-ignited energetic materials: I. Fundamental mechanisms and processes. IEEE Trans Plasma Sci 43(12):3999–4008

Han R, Wu J, Qiu A et al (2018) Electrical explosions of Al, Ti, Fe, Ni, Cu, Nb, Mo, Ag, Ta, W, W-Re, Pt, and Au wires in water: a comparison study. J Appl Phys 124(4):043302

Hao H (2019) Experimental study on electrical explosion characteristics of metal wire and its application in rock breaking. Northeastern University

Hollandsworth CE, Powell JD, Keele MJ, et al (1998) Conduction in electrically exploded wires of nonuniform diameters. NASA (19990025763)

Hu Z, Cao Z, Li S et al (2021) Fluid-structure interaction between a high-pressure pulsating bubble and a floating structure. Chin J Theor Appl Mech 53(04):944–961

Huang C, Subhash G, Vitton SJ (2002) A dynamic damage growth model for uniaxial compressive response of rock aggregates. Mech Mater 34(5):267–277

Ji N, Pei Y, Yan K et al (2012) Development of high-voltage pulse-transmission electric cable for plasma drill. Mach Electron 8:7–10

Jia L, Peng S, Xu J et al (2022) Novel multi-field coupling high-voltage electric pulse fracturing coal–rock permeability enhancement test system. Int J Rock Mech Min 158:105180

Jiang Y, Xian X, Yi J et al (2008) Experimental and mechanical on the features of ultrasonic vibration stimulating the desorption of methane in coal. J China Coal Soc 33(6):675–680 (**(in Chinese)**)

Jigna X, Jun X, Guanhua N et al (2020) Effects of pulse wave on the variation of coal pore structure in pulsating hydraulic fracturing process of coal seam. Fuel 264:116906

Jin Y (2014) Study on radiation ignition and combustion characteristics of solid propellant by electrothermal plasma. Nanjing University of Science & Technology

Kovalchuk BM, Kharlov AV, Vizir VA et al (2010) High-voltage pulsed generator for dynamic fragmentation of rocks. Rev Sci Instrum 81(10):103506

Kovalchuk BM, Kharlov AV, Kumpyak EV et al (2013) High-voltage pulsed generators for electro-discharge technologies. J Instrum 8(09):P09012

Kuszmaul JS (1987) A new constitutive model for fragmentation of rock under dynamic loading. Sandia National Labs, Albuquerque, NM, 6527538

Kutter HK, Fairhurst C (1971) On the fracture process in blasting. Int J Rock Mech Min Sci Geomech Abst 8(3):181–202

Li H, Li B, Li H (2007) Experimental study on gun performance augmentation by plasma. J Project Rockets Missiles Guidance 02:297–299+312

Li H (2015) Fracturing and permeability increasing behavior and mechanism of coal rock by electric pulse stress wave. China University of Mining and Technology, Xuzhou

Li H, Qin Y, Zhang Y (2015) Experimental study on the effect of strong repetitive pulse shockwave on the pore structure of fat coal. J China Coal Soc 40(04):915–921

Li M, Li H, Luo X (2019a) Test of controllable shock wave technology to enhance coal seam gas extraction in Linhua Coal Mine. China Coal 45(08):54–57

Li S, Zhang A, Han R (2019b) The Mechanism of jetting behaviors of an oscillating bubble. Chin J Theor Appl Mech 51(06):1666–1681

Li P, Zhang X, Li H (2021) Technology of coupled permeability enhancement of hydraulic punching and deep-hole pre-splitting blasting in a" three-soft" coal seam. J Mater Sci Technol 55(1):89–96

Li C, Nie B, Zhang Z et al (2022a) Experimental study of the structural damage to coal treated by a high-voltage electric pulse discharge in water. Energ Fuel 36(12):6280–6291

Li Y, Ma H, Zhang Y, et al (2022b) Laboratory experimental study on controllable shock wave fracturing casing well reservoir. Journal of Yan'an University (Natural Science Edition) 41(04): 56–61

Li W, Zhang Y, Wang D et al (2023) Theoretical basis and technical method of permeability enhancement of tectonic coal seam by high intensity acoustic wave in situ. Processes 11(8):2372

Li P, Jin F (1994) Calculation of shock wave and plasma parameters in liquid discharge. J Zhejiang Univ (Nat Sci) 01:27–35

Li J (2010) Study on gas desorption and emission characteristics of coal under the action of acoustic wave. Anhui University of Science & Technology

Li D (2011) Mechanism and experimental study of high voltage pulse discharge pile expansion. Jilin University

Li B (2022) Experimental study on mechanism of high voltage electric pulse pressure fracturing coal body. Anhui University of Science & Technology

Liu X, Feng C, Zhu Z et al (1999) Study on optical radiation of high voltage pulse discharge in water. J Beijing Inst Technol 01:12–16

Liu B, Huang J, Wang Z et al (2009) Study on damage evolution and acoustic emission character of coal-rock under uniaxial compression. Chin J Rock Mech Eng 28(S1):3234–3238

Liu Q, Ding W, Han R et al (2017) Fracturing effect of electrohydraulic shock waves generated by plasma-ignited energetic materials explosion. IEEE Trans Plasma Sci 45(3):423–431

Liu T, Liu S, Lin B et al (2020) Stress response during in-situ gas depletion and its impact on permeability and stability of CBM reservoir. Fuel 266:117083

Liu T, Lin B, Fu X et al (2021) Modeling coupled gas flow and geomechanics process in stimulated coal seam by hydraulic flushing. Int J Rock Mech Min 142:104769

Liu Z, Lin X, Wang Z et al (2022) Modeling and experimental study on methane diffusivity in coal mass under in-situ high stress conditions: a better understanding of gas extraction. Fuel 321:124078

Lu H (2015) Experimental study on fracturing effect of high voltage electric pulse on coal body. China University of Mining And Technology, Beijing

Lu X, Pan Y, Zhang H (2002) Calculation of shock wave and plasma parameters in liquid discharge. Acta Phys Sin-Ch Ed 07:1549–1553

Lu Y, Liu Y, Li X et al (2010) A new method of drilling long boreholes in low permeability coal by improving its permeability. Int J Coal Geol 84(2):94–102

Lu W, Yang J, Yan P et al (2012) Dynamic response of rock mass induced by the transient release of in-situ stress. Int J Rock Mech Min 53:129–141

Luo M, Yang L, Wen H, et al (2022) Numerical optimization of drilling parameters for gas predrainage and excavating-drainage collaboration on roadway head. Geofluids 3241211

Maurel O, Reess T, Matallah M et al (2010) Electrohydraulic shock wave generation as a means to increase intrinsic permeability of mortar. Cement Concrete Res 40(12):1631–1638

Mu C (2012) Model experimental study on crack propagation of coal under the coupling effect of explosion load and ground stress. J Exp Mech 27(04):511–516
Mu C, Pan F (2013) Numerical simulation of crack propagation in coal under the coupling effect of explosion load and ground stress. Chin J High Pressure Phys 27(03):403–410
Oreshkin VI, Chaikovsky SA, Ratakhin NA et al (2007) "Water bath" effect during the electrical underwater wire explosion. Phys Plasmas 14(10):102703
Oshita D, Hosseini SHR, Miyamoto Y et al (2013) Study of underwater shock waves and cavitation bubbles generated by pulsed electric discharges. IEEE Trans Dielect El in 20(4):1273–1278
Peng C (2016) Development of high-voltage pulse rock breaking device. Huazhong University of Science and Technology
Qin Y, Hengle L I, Yongmin Z, et al (2021) Numerical analysis on CSW fracturing behavior of coal seam under constraint of geological and engineering conditions. Coal Geol Explor (1):108–118, 129
Qiu A, Zhang Y, Kuai B, et al (2012) Application of high power pulse technology in unconventional natural gas development. In: Proceedings of the Second Energy Forum of China Academy of Engineering/National Energy Administration. Beijing: Coal Industry Press, 22–24
Rao P, Ouyang P, Nimbalkar S et al (2022) Mechanism analysis of rock failure process under high-voltage electropulse: analytical solution and simulation. Materials 15(6):2188
Rososhek A, Efimov S, Goldman A et al (2019) Microsecond timescale combustion of aluminum initiated by an underwater electrical wire explosion. Phys Plasmas 26(5):053510
Sasaki T, Yano Y, Nakajima M et al (2006) Warm-dense-matter studies using pulse-powered wire discharges in water. Laser Part Beams 24(3):371–380
Seidle JP, Huitt LG (1995) Experimental measurement of coal matrix shrinkage due to gas desorption and implications for cleat permeability increases. SPE International Oil and Gas Conference and Exhibition in China. SPE SPE-30010-MS
Shi H, Fan Y, Yin G et al (2021a) Experimental study on underwater electrical explosion of copper wires with varied diameter and length. High Voltage Eng 47(07):2599–2606
Shi H, Hu Y, Li T, et al (2021b) Detonation of a nitromethane-based energetic mixture driven by electrical wire explosion. J Phys D Appl Phys 55(5):05LT01
Su S (2020) Application of controllable shock wave for permeability enhancement in hard thick coal seam. Coal Eng 52(09):71–75
Su S, Zhang Y, Li W et al (2021) Application of controllable shock wave antireflection technology in soft coal seam with low porosity and low permeability in Jining. China Mining Mag 30(05):173–179
Sultanov MA, Oleinikov VP (1976) Gasdynamic acceleration in the compression zone of intersecting plasma streams. Sov Phys-Tech Phys (Engl Transl) (United States) 21(8)
Sun B (2013) Discharge plasma in liquid and its applications. Science Press, Beijing
Sun Y, Fu R, Fan A, et al (2015) Study of rock fracturing generated by pulsed discharging under confining pressure. 2015 IEEE Pulsed Power Conference (PPC). IEEE, pp 1–4
Suo Y (2005) Study for macro-damage degree of weakening blast in hard top-coal. Rock Soil Mech 26(6):893–895
Tao J, Yang X, Li H et al (2020) Effects of in-situ stresses on dynamic rock responses under blast loading. Mech Mater 145:103374
Taylor LM, Chen EP, Kuszmaul JS (1986) Microcrack-induced damage accumulation in brittle rock under dynamic loading. Comput Method Appl M 55(3):301–320
Thorne BJ, Hommert PJ, Brown B (1990) Experimental and computational investigation of the fundamental mechanisms of cratering. Sandia National Lab. (SNL-NM), Albuquerque, NM (United States) 6813604
Touya G, Reess T, Pecastaing L et al (2006) Development of subsonic electrical discharges in water and measurements of the associated pressure waves. J Phys D Appl Phys 39(24):5236
Tucker TJ (1961) Behavior of exploding gold wires. J Appl Phys 32(10):1894–1900
Tucker TJ, Toth RP (1975) EBW1: A computer code for the prediction of the behavior of electrical circuits containing exploding wire elements. Sandia National Lab. (SNL-NM), Albuquerque, NM (United States)
Vahitov, Simkin, Cai T (1993) Exploiting oil from strata by physical field. Petroleum Industry Press
VanDevender JP (1978) The resistive phase of a high-voltage water spark. J Appl Phys 49(5):2616–2620
Wang Z (2020) Application of controllable shock wave plugging removal and permeability improvement technology in CBM gas field of Southern Yanchuan. Reserv Eval Develop 10(04):87–92
Wang E, Kong X, He X et al (2019) Dynamics analysis and damage constitute equation of triaxial coal mass under impact load. J China Coal Soc 44(7):2049–2056
Wang Q, Su Y, Jiang A et al (2021) Experimental research on the technology of permeability enhancement and plug removal by controllable shockwave. Natural Gas Oil 39(02):68–74
Wang X, Li W (2019) Application analysis of controlled shock wave antireflection technology in Jining Coal Mine. Shanxi Coking Coal Sci Technol 43(02):4–7+11
Xiao S, Su L, Jiang Y et al (2019) Numerical analysis of hard rock blasting unloading effects in high in situ stress fields. B Eng Geol Environ 78:867–875
Xiao B, Guo D, Li S, et al (2024) Rare earth elements (REEs) characteristics of shales from Wufeng-Longmaxi Formations in deep buried area of the northern Sichuan Basin, Southern China: Implications for provenance, depositional conditions and paleoclimate. ACS Omega. https://doi.org/10.1021/acsomega.3c03086
Xie H, Ju Y, Li L (2005) Criteria for strength and structural failure of rocks based on energy dissipation and energy release principles. Chin J Rock Mech Eng 17:3003–3010
Xu L, Fan C, Luo M et al (2023) Elimination mechanism of coal and gas outburst based on geo-dynamic system with stress–damage–seepage interactions. Int J Coal Sci Techn 10(1):74
Xun T, Yang H, Zhang J et al (2010) Numerical simulation and experimental study of accelerator electric water hammer. High Power Laser Part Beams 22(02):425–429
Yan D, Bian X, Que M (2014) Basic phenomenon analysis of high voltage discharge in water. Coal Technol 33(07):294–296
Yan F, Lin B, Zhu C et al (2016) Experimental investigation on anthracite coal fragmentation by high-voltage electrical pulses in the air condition: effect of breakdown voltage. Fuel 183:583–592
Yan F, Lin B, Xu J et al (2018) Structural evolution characteristics of middle–high rank coal samples subjected to high-voltage electrical pulse. Energ Fuel 32(3):3263–3271
Yan F, Xu J, Lin B et al (2019) Changes in pore structure and permeability of anthracite coal before and after high-voltage electrical pulses treatment. Powder Technol 343:560–567
Yan Z, Ma G, Zhang W (2021) Gas (oil-type gas) control technology and new management mode in Huangling mining area. Shaaxi Coal 40(03): 26–32+50
Yang L, Ding C (2018) Fracture mechanism due to blast-imposed loading under high static stress conditions. Int J Rock Mech Min 107:150–158
Yang J, Gao W (2000) Experimental study on damage properties of rock under dynamic loading. J Heilongjiang Min Inst 01:50–53
Yang J, Wang S (1996) Study on fractal damage model of rock blasting. Explosion and Shock Waves 16(1):5–10

Yang R, Ding C, Li Y et al (2019) Crack propagation behavior in slit charge blasting under high static stress conditions. Int J Rock Mech Min 119:117–123

Yang W, Zheng C, Li A et al (2020) Feasibility analysis of controllable shock wave fracturing offshore oil layer. Drill Prod Technol 43(01):38–41+9

Yang L, Fan C et al (2023a) An improved gas–liquid–solid coupling model with plastic failure for hydraulic flushing in gassy coal seam and application in borehole arrangement. Phys Fluids 35:036603

Yang L, Fan C, Wen H et al (2023b) An improved gas–liquid–solid coupling model with plastic failure for hydraulic flushing in gassy coal seam and application in borehole arrangement. Phys Fluids 35:036603

Yao B, Ma Q, Wei J et al (2016) Effect of protective coal seam mining and gas extraction on gas transport in a coal seam. Int J Coal Sci Techn 26(4):637–643

Yao W, Zhou H, Han R et al (2019) An empirical approach for parameters estimation of underwater electrical wire explosion. Phys Plasmas 26(9):093502

Zhang F, Peng J, Qiu Z et al (2017a) Rock-like brittle material fragmentation under coupled static stress and spherical charge explosion. Eng Geol 220:266–273

Zhang Y, Qiu A, Qin Y (2017b) Engineering practice of controllable shock wave anti-reflection soft coal seam. Shanxi Coking Coal Sci Technol 41(Z1):116–121

Zhang Y, Qiu A, Qin Y (2017c) Principle and engineering practices on coal reservoir permeability improved with electric pulse controllable shock waves. Coal Sci Technol 45(9):0253–2336

Zhang X, Lin B, Zhu C et al (2019a) Petrophysical variation of coal treated by cyclic high-voltage electrical pulse for coalbed methane recovery. J Petrol Sci Eng 178:795–804

Zhang Y, An S, Chen D, et al (2019b) Preliminary tests of coal reservoir permeability enhancement by controllable shock waves in baode coal mine 8# coal seam. Saf Coal Mines 50(10): 14–17+21

Zhang Y, Meng Z, Qin Y et al (2019c) Innovative engineering practice of soft coal seam permeability enhancement by controllable shock wave for mine gas extraction: a case of Zhongjing Mine, Shuicheng, Guizhou Province. J China Coal Soc 44(08):2388–2400

Zhang Y, Yao W, Qiu A et al (2019d) Review of wire electrical explosion phenomena. High Voltage Eng 45(08):2668–2680

Zhang D, Zhang Y, Li J et al (2023a) Application of controllable shock wave seam permeability enhancement in cross-seam drilling. Coal Eng 55(06):73–78

Zhang S, Chen M, Zhang X et al (2023b) Application of controllable shock wave to increase coal seam permeability. Coal Technol 42(09):129–133

Zhao L (2022) Mechanism of permeability enhancement in coal under repetitive strong shock waves. Arab J Geosci 15(3):222

Zheng C, Kizil M, Chen Z et al (2017) Effects of coal damage on permeability and gas drainage performance. Int J Min Sci Technol 27(5):783–786

Zhou X (2010) Dynamic damage constitutive relation of mesoscopic heterogenous brittle rock under rotation of principal stress axes. Theor Appl Fract Mec 54(2):110–116

Zhou X, Li X (2009) Constitutive relationship of brittle rock subjected to dynamic uniaxial tensile loads with microcrack interaction effects. Theor Appl Fract Mec 52(3):140–145

Zhou J, Jiang T, Zhang B et al (2014) Preliminary study on high-energy pulsed arc fracturing. Pet Drill Tech 42(03):76–79

Zhou H, Han R, Liu Q et al (2015a) Generation of electrohydraulic shock waves by plasma-ignited energetic materials: II. Influence of wire configuration and stored energy. IEEE Trans Plasma Sci 43(12):4009–4016

Zhou H, Han R, Wu J (2015b) Model and simulation study of discharge channel during underwater Cu wire explosion. High Voltage Eng 41(09):2943–2949

Zhou H, Zhang Y, Li H et al (2015c) Generation of electrohydraulic shock waves by plasma-ignited energetic materials: III. Shock wave characteristics with three discharge loads. IEEE Trans Radiat Plasma 43(12):4017–4023

Zhou X, Qin Y, Li H, et al (2015d) Formation and development of coal micro-fractures under stress wave induced by electrical impulses. Coal Sci Technol 43(02):127–130+143

Zhou H, Zhang Y, Han R et al (2016) Signal analysis and waveform reconstruction of shock waves generated by underwater electrical wire explosions with piezoelectric pressure probes. Sensors-Basel 16(4):573

Zhou H (2017) Study on shock wave generation mechanism and energy conversion characteristics of microsecond electrical explosion of copper wire in water. Xi'an Jiaotong University, Xi'an

Zingerman Z (1956) Pressure on the shockwave front from the slope impulse energy in an electric discharge. Zh Tekh Fiz 26(11):2539–2540

Zuo Q, Disilvestro D, Rich ter JD (2010) A crack-mechanics based model for damage and plasticity of brittle materials under dynamic loading. Int J Solids Struct 47(20):2790–2798

Publisher's Note Springer Nature remains neutral with regard to jurisdictional claims in published maps and institutional affiliations.